AFCRL-71-0235
16 APRIL 1971
ENVIRONMENTAL RESEARCH PAPERS, NO. 352

AIR FORCE CAMBRIDGE RESEARCH LABORATORIES
L. G. HANSCOM FIELD, BEDFORD, MASSACHUSETTS

A Remote-Sensing Investigation of Four Mojave Playas

C.E. MOLINEUX
E.E. BLIAMPIS
J.T. NEAL, MAJ, USAF

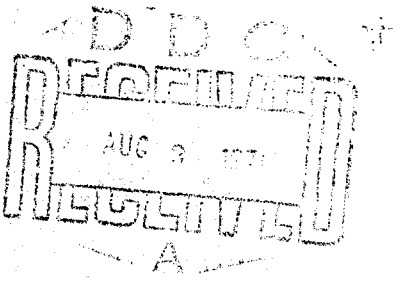

AIR FORCE SYSTEMS COMMAND
United States Air Force

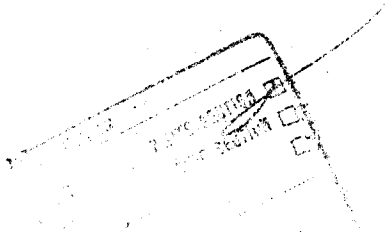

Unclassified
Security Classification

DOCUMENT CONTROL DATA - R&D

(Security classification of title, body of abstract and indexing annotation must be entered when the overall report is classified)

1. ORIGINATING ACTIVITY *(Corporate author)* Air Force Cambridge Research Laboratories (LW) L. G. Hanscom Field Bedford, Massachusetts 01730	2a. REPORT SECURITY CLASSIFICATION Unclassified 2b. GROUP

3. REPORT TITLE

A REMOTE-SENSING INVESTIGATION OF FOUR MOJAVE PLAYAS

4. DESCRIPTIVE NOTES *(Type of report and inclusive dates)*

Scientific. Interim.

5. AUTHOR(S) *(First name, middle initial, last name)*

Carlton E. Molineux
Emmanuel E. Bliamptis
James T. Neal, Maj USAF

6. REPORT DATE 16 April 1971	7a. TOTAL NO. OF PAGES 70	7b. NO. OF REFS 21
8a. CONTRACT OR GRANT NO. LDF (Partially) b. PROJECT, TASK, WORK UNIT NOS. 7628-01-01 27-64 c. DOD ELEMENT 62101F d. DOD SUBELEMENT 681000	9a. ORIGINATOR'S REPORT NUMBER(S) AFCRL-71-0235 9b. OTHER REPORT NO(S) *(Any other numbers that may be assigned this report)* ERP No. 352	

10. DISTRIBUTION STATEMENT

1-This document has been approved for public release and sale; its distribution is unlimited.

11. SUPPLEMENTARY NOTES This research was partially supported by the Air Force In-House Laboratory Independent Research Fund.	12. SPONSORING MILITARY ACTIVITY Air Force Cambridge Research Laboratories (LW) L. G. Hanscom Field Bedford, Massachusetts 01730

13. ABSTRACT—Dry lakebeds (playas) in the Mojave Desert are often hard and flat enough to serve as natural landing areas for aircraft. However, the surface physical properties of moisture, strength, and microrelief can vary with seasonal or local conditions. It is desirable to develop methods for determining and monitoring these properties and their variations. Airborne remote sensing enables collection of data on the reflectance, temperature, and emissivity of these surfaces that can be correlated with soil parameters. Four playas in the Mojave Desert that have a variety of surface properties were investigated. Airborne spectrophotography and thermal infrared imagery were obtained by overflights. Ground photometry and measurements of surface properties were obtained. Moisture-sensitive dyes were applied to one lakebed surface to evaluate the feasibility of monitoring its dryness through color changes apparent on the aerial photography. The report describes the results of the remote-sensing investigations and the correlation of photographic and imagery interpretation with actual surface conditions. Such soil properties as moisture, density, and composition can be identified by their spectral reflectance variations apparent on aerial or ground imagery. Spectrophotography and thermal infrared imagery are particularly useful in discrimination of soft or wet surfaces as opposed to hard or dry surfaces. Variability of solar illumination is a limiting factor in applying such remote-sensing techniques.

DD FORM 1 NOV 68 1473

Unclassified
Security Classification

Unclassified

Security Classification

14. KEY WORDS	LINK A		LINK B		LINK C	
	ROLE	WT	ROLE	WT	ROLE	WT
Aerial photography						
Aircraft landing areas						
Bearing strength						
Earth Sciences						
Geology						
Infrared						
Landforms						
Military geographic information						
Mojave desert						
Passive microwave						
Photography						
Photometry						
Playas						
Reflectance						
Remote sensing						
Soils						
Soil moisture						
Terrain parameters						
Spectrophotography						

Unclassified

Security Classification

AFCRL-71-0235
16 APRIL 1971
ENVIRONMENTAL RESEARCH PAPERS, NO. 352

TERRESTRIAL SCIENCES LABORATORY PROJECT 7628 ILIR

AIR FORCE CAMBRIDGE RESEARCH LABORATORIES
L. G. HANSCOM FIELD, BEDFORD, MASSACHUSETTS

A Remote-Sensing Investigation of Four Mojave Playas

C.E. MOLINEUX
E.E. BLIAMPTIS
J.T. NEAL, MAJ, USAF *

*USAF Academy, Colorado

This research was partially supported by the Air Force In-House Laboratory Independent Research Fund.

AIR FORCE SYSTEMS COMMAND
United States Air Force

Abstract

Dry lakebeds (playas) in the Mojave Desert are often hard and flat enough to serve as natural landing areas for aircraft. However, the surface physical properties of moisture, strength, and microrelief can vary with seasonal or local conditions. It is desirable to develop methods for determining and monitoring these properties and their variations. Airborne remote sensing enables collection of data on the reflectance, temperature, and emissivity of these surfaces that can be correlated with soil parameters. Four playas in the Mojave Desert that have a variety of surface properties were investigated. Airborne spectrophotography and thermal infrared imagery were obtained by overflights. Ground photometry and measurements of surface properties were obtained. Moisture-sensitive dyes were applied to one lakebed surface to evaluate the feasibility of monitoring its dryness through color changes apparent on the aerial photography. The report describes the results of the remote sensing investigations and correlation of photographic and imagery interpretation with actual surface conditions. Such soil properties as moisture, density, and composition can be identified by their spectral reflectance variations apparent on aerial or ground imagery. Spectrophotography and thermal infrared imagery are particularly useful in discrimination of soft or wet surfaces as opposed to hard or dry surfaces. Variability of solar illumination is a limiting factor in applying such remote-sensing techniques.

Contents

Illustrations

Maps

Tables

FRONTISPIECE: Aerial View, Looking East, of the Playa in Harper Valley, California. Dark areas in center foreground are moist zones that resulted from irrigation runoff. The northern vegetated dune area (left) has similar reflectance to the barren playa, but hard clay zones appear lighter. The hard clay area on the southern edge (right center) also appears lighter than the adjacent soft, dry, friable surfaces that were predominant. Nov. 1962, USAF photo.

A Remote-Sensing Investigation of Four Mojave Playas

1. INTRODUCTION

Dry lakebeds (playas) are perhaps the hardest and flattest of natural landing fields, but a consideration that has hindered their potential utility is the fact that their surface physical properties (soil moisture and salinity, strength, microrelief) vary with time. Often these changes are pronounced and occur over short intervals, such as following a rain or dust storm (Neal et al, 1968). Marked variations in soil strength can be observed over a period of several years.

Thus it is desirable to develop methods for determining surface changes without having to perform costly and time-consuming resurveys by conventional ground-based methods. Airborne remote sensing appears to be one method that holds promise for observing these changes (Bliamptis, 1967). The diversity of techniques presently available makes it possible to obtain a range of data on reflectance, temperature, and emissivity that may reveal information on the soil parameters of interest.

Four playas in the Mojave Desert, California (Figure 1), that possess a variety of surface properties were selected for study, and remote-sensor overflights were conducted in September 1967. Infrared thermal imagery, spectrophotography, color and false-color photography, and infrared and conventional black-and-white

(Received for publication 9 April 1971)

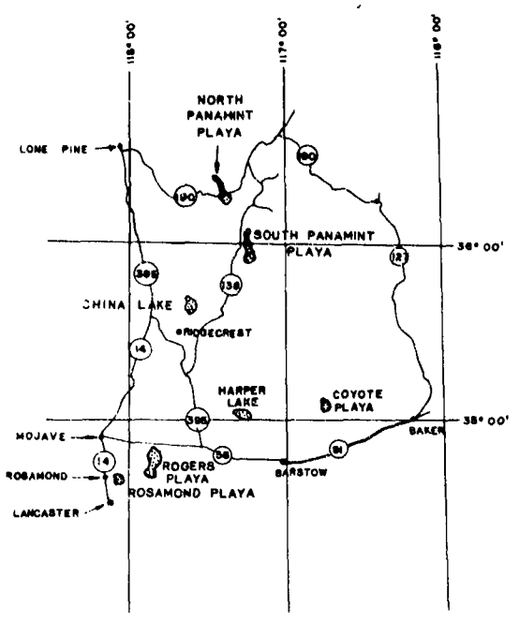

Figure 1. Locations of the Playas Studied

photography were obtained during the mission. Ground measurements of actual conditions were taken during the overflights.

Soil moisture is a critical parameter that is directly related to soil strength. Because of its importance, and because of past difficulty in its measurement, the use of moisture-sensitive chemical dye agents was considered. One such agent, cobaltous chloride, was sprayed on a lakebed surface at places having a range of soil moisture contents. The tests were conducted simultaneously with the remote-sensor overflights.

Harper, Coyote, and North and South Panamint dry lakes (playas) contain a range of surface conditions that include the following: (1) hard, dry crusts; (2) hard evaporite crusts; (3) soft, sticky-wet surfaces; (4) soft, dry, friable surfaces; (5) giant desiccation cracks; (6) vegetation mounds; (7) sand accumulations; (8) miscellaneous wheel ruts and cultural modifications. These are the principal playa surface variations of significance.

This report describes results of remote sensing and dye application tests, and suggests methods of monitoring surface properties through their employment. Most of the effort was concentrated on Harper and Coyote, two large and geographically accessible playas.

2. SURFICIAL GEOLOGIC PROPERTIES OF THE PLAYAS

2.1 Harper

The playa is the site of former pluvial Lake Harper, an apparently isolated lake that received its water from overflow of the Mojave River during the Pleistocene period. Alluvial slopes rise gradually in all directions from the playa. The north and east slopes are slightly steeper, reaching low basalt-covered mountains within a few miles. On the west and south no mountains appear; the land rises gently for over 10 miles. The slopes are pediment slopes with an alluvial cover.

The alluvium increases approaching the lakebed; sediments beneath the playa are as much as 1200 ft deep.

The north side of the playa is covered with sand dunes, at times reaching heights of 15 ft, although most are 5 ft or less. The playa is a compound type, with zones of hard, dry clay and puffy "self-rising" ground, the latter being predominant in recent years. Extensive flooding during 1965-6 converted much of the playa to a hard, dry crust. Additionally, capillary discharge of ground water has deposited varying amounts of salt and other evaporites at the surface. There is not a well-developed soil profile as such; however, where saline ground water deposits evaporites, a marked zonation exists.

Surface soils on the barren part of the playa are diverse in character, but they can be grouped into two major categories, with several others transitional between the two. The major types reflect surface and subsurface hydrologic conditions: (1) hard, dry clay, and (2) soft, friable ground. Ground water is discharged from the latter through capillary rise and there is subsequent evaporation. Figures 2 and 3 are representative surface views of each soil type.

Hard, dry clay is present over the majority of the playa. Soil mud cracks are typically well-defined, flat, and of small to medium size (Figure 2). They may be raised in places and they may also appear as transitional phases with self-rising ground. The southern dry clay area may actually be moist at the surface; this

Figure 2. Surface View of Typical Hard Clay Playa Soil

Figure 3. Surface View of Typical Puffy Soil

moisture is derived from irrigation runoff from nearby fields and should not be confused with capillary water.

Soft, friable surfaces were present in the east-central portion of the playa and in the southern and western edges. They displayed a diversity of forms. Salt stains and thin salt crusts were common in the eastern part. It was lumpy in places (Figure 3) with an irregular appearance or it was relatively flat. These variations are caused by standing water following a rainfall wherein the surface is levelled. This type of surface is a dry, puffy, clay-silt that has low bulk density and low strength to a depth of 6 or 8 in. Below this depth the soil is moist and highly plastic. Shallow-lying ground water beneath this playa is usually 15 ft or less below the surface, but intensive pumping for irrigation has created a depression in the deeper-lying ground water south of the playa.

2.2 Coyote

Coyote playa occupies the central portion of the valley in which it is located. The extent of the clays beneath encroaching alluvial fan materials and the shoreline features on the adjacent alluvial slopes indicate that during late Pleistocene time a lake occupied an area larger than that of the present playa.

The playa surface is essentially flat, except along the margins where there is a gentle slope. Small washes and gullies entering the playa have cut into the clays on these slopes, producing a relief of as much as 2 ft, but in the center of the playa dissection of the sediments is negligible. In areas where different surface types are produced by the different types of clays, soft, puffy surfaces stand above hard surfaces by as much as a foot.

Giant desiccation fissures, occurring either as open cracks or as outlines, can be seen in all parts of the playa. Associated with relict outlines are plant mounds and ridges up to several feet in height. Drain holes are commonly found at the intersection of desiccation fissures (Neal, et al, 1968).

The playa has two basic types of surface: a hard, compact surface and a soft, friable surface, with intermediate types transitional between these two. Continuously hard areas are located in the central and northern sections of the playa, although some portions of the northern section develop friable or "puffy" conditions. Generally, areas of hard surface show little or no relief, and the clay has a very smooth surface covered with a system of fine irregular cracks that form polygons measuring 3 to 4 in. across. In the northern section, clays are consistently coarser in texture, slightly darker in color, and have wider cracks forming 1-ft polygons. Coarse deposits of pebbles and cobbles are common, but they are strewn loosely on the surface of the hard clay and are not buried or deeply embedded. The playa is underlain by poorly permeable clays that prevent the flow

of ground water through this portion of the basin. The upper sediments, therefore, generally remain hard and dry.

Areas of puffy surface are characterized by a thin, uneven, and easily broken crust underlain by a layer of fine, dry, loose material. Beneath this, the sediments are firm and compact. The color of the crust and underlying loose material is light brown, darker than the color of the hard clay surface. In many places the crust is broken by thin, irregular cracks. This condition is caused primarily by the addition of moisture to the clay, its source being ground water moving upward by capillary rise. Some patchy areas of puffy surface are continually undergoing change and may occur alternately in a hard or a puffy condition. These changes are often the result of surficial flooding.

2.3 North Panamint

The playa is situated in a north-south trending graben lying between the Panamint Range on the east and the Argus Range on the west. The north end of the valley is bounded by a complex upthrust of crystalline rocks, while the hills forming its west side are a complex of extrusive volcanics. The south end of the valley is formed by the coalescence of alluvial fans from the east and west sides, while its floor is a flat plain surrounded by encroaching alluvial fans. There is a high rock outcrop at the east edge of the northern part of the playa. This, together with beach deposits higher up on the west slope, the truncated hills facing the playa, and the eroded alluvial fans on the north end, indicates that most of the area was developed under water during the Pleistocene period.

The playa surface consists predominantly of hard, dry crust and discharges little or no ground water. It is underlain mainly by silts and clays. The playa is crossed by a series of shallow stream channels up to 12 in. in depth. Its surface is mud-cracked to a depth of several inches, with a sparse growth of xerophytic brush often found outlining giant desiccation fissures. About one-third of the total area is covered with sand, gravel, and cobbles of vesicular lava. The surface not covered by the gravel material is a hard, yellow-brown, calcareous sandy clay. This same material underlies the gravel. There is little change in the soil material from the surface to a depth of 10 ft. Beneath this depth lie moist lacustrine clays of pluvial Lake Panamint.

2.4 South Panamint

The lakebed lies on a north-south graben of young basin range with an easterly tilt. The east side of the valley is formed by sharply folded sedimentary carbonates and argillites, covered with a veneer of eroded extrusive volcanics. The south end of the valley is formed by a transverse fault trending northeast to southwest. There is negligible dissection in the flatter area of the playa, but a few small drainage ditches exist on the outside of the area.

The playa can be termed a wet playa, as it discharges much ground water and is underlain mainly by coarse silts and sands. This is in contrast to North Panamint playa that discharges little or no ground water and is rich in fine clay at depth.

The surface consists of flat, mud-cracked, clayey silt with random patches of blister salt crust. The only microrelief features in the area are ruts made by ground vehicles and landing aircraft. There is a landing strip at the south end. The soil material from the surface to the water table is a tan silty clay with salts. The top 6 to 9 in. contains the same material, except for a heavier concentration of salts, calcareous silt, and some fine sand. In some areas the crust is very hard because of chemical cementation, presumably calcium carbonate.

Large areas of the playa become encrusted with salt during the summer. These evaporite deposits are susceptible to wind erosion since they are above the saturated zone and dry into flakes and shards.

3. REMOTE-SENSING INVESTIGATIONS

3.1 Aerial-Sensing Techniques

Aerial photography and imagery of the four playas (Harper, Coyote, North Panamint, South Panamint) were obtained at an altitude of 10,000 ft above each area from an instrumented C-47 aircraft. In addition, passive microwave and infrared radiometric studies of Harper playa were conducted in March 1967, but airborne sensing was not accomplished at that time.

The airborne sensing comprised black-and-white photography in a 9 in. x 9 in. format and nine-band multispectral photography in a 70-mm format for all four dry lakebeds. In addition, 9 in. x 9 in. Ecktachrome photography was taken over Harper and North and South Panamint playas, and 9 in. x 9 in. infrared Ektachrome photography was taken over Harper and Coyote playas.

The multispectral camera (Molineux, 1965) had its spectral bandwidths chosen to optimize the characteristic reflectance of soil and natural materials. Table 1 lists the bands used for these investigations. They were obtained by narrow-bandpass filters incorporated into each lens of the camera.

Day and night thermal infrared scanning imagery in the 3.5 to 5.5 μm region was obtained at the same altitude over all areas, simultaneously with the aerial photography during the day and independently at night. Imagery was recorded from the scanner on 70-mm film and magnetic tape for later analysis.

Concurrently with the airborne-sensing overflights, the physical properties of the dry lakebeds were determined by a field party. Extensive photometric measurements of the reflectance of each area and pertinent surface anomalies

Table 1. Multispectral Camera Wavelength Bands

Lens No.	Bandwidth (nm)
1	385 - 450 (with vertical polarization)
2	385 - 450 (with horizontal polarization)
3	440 - 525
4	505 - 570
5	550 - 625
6	615 - 690
7	700 - 890
8	755 - 890
9	790 - 890

were made with a photometer equipped with narrow-band filters duplicating those used in the aerial multispectral camera. Soil moisture content, soil and air temperatures, and soil hardness were measured and samples obtained for later laboratory analysis and spectral reflectance measurement. Visual observation and ground photography were made of surface conditions relevant to interpretation of the aerial imagery.

The general procedure was to lay out a traverse along the main area of the dry lakebed to cover a wide range of soil and moisture conditions. The aerial photography and imagery flight lines covered all of the investigation points along this traverse and also selected anomalies to either side.

3.2 Passive Microwave Measurements

Moisture content and its interaction with the physical and chemical properties of soil is the dominant factor in soil strength and trafficability. For this reason, the determination or estimation of the presence and extent of soil moisture, as apparent from remote-sensing readout, was the main objective of the study.

For the passive microwave radiometric survey of Harper playa, conducted by personnel of the Space Division, Aerojet-General Corporation, two radiometers (13.4 GHz and 37 GHz), each operating simultaneously with both horizontal and vertical polarization capability, were used. The system was mounted atop a 16 ft (5 m) boom on a ground vehicle, allowing for continuous measurements in the elevation plane from 0° to 180°. Figure 4 shows the vehicle-mounted system.

Radiometric brightness temperatures were measured along a complete 8 km (5 mile) traverse across the lakebed and at many selected anomalies of soil type and moisture. Correlation of measured radiometric temperatures with soil

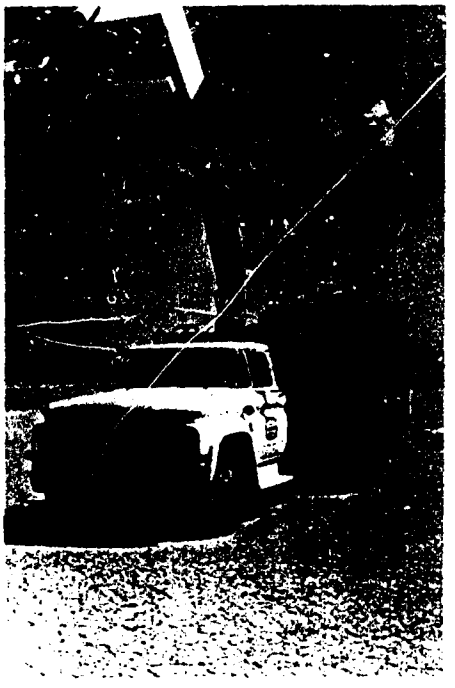

Figure 4. Microwave Survey Vehicle

moisture and soil strength measurements was made through a 60 cm profile of the playa. The data, shown in Figures 5 and 6, indicate that microwave radiometric temperature is a function of soil moisture content for both horizontal and vertical polarization. An increase in moisture causes a decrease in radiometric temperature. As the moisture content increases, the difference between horizontal and vertical polarization radiometric temperatures also increases (Aerojet-General Corp., 1968).

The general relationship derived from the data show that a 1 percent increase in soil moisture results in a decrease in radiometric temperature of 4K to 5K, leading to the conclusion that it is possible to determine small variations in soil moisture by using state-of-the-art microwave radiometers (Kennedy and Edgerton, 1968). Such optimism must be tempered by the realization that the effect of soil temperature variations must be removed from the microwave temperature measurement interpretations and that such interpretations are complex functions of the effective dielectric constant of the soil-water system.

Soil strength measurements also showed a good correlation with radiometric temperatures, particularly with the 13.4 GHz measurements, at depths below 6 in. Near-surface strength measurements do not show much correlation, except in obvious puffy or very moist areas. These conclusions illustrate the difference in "penetration" of the two radiometers used for the measurements. The 13.4-GHz sensor had a wavelength of 2.2 cm and was more strongly influenced by the product of the moist sediments beneath the dry puffy crust than was the 37-GHz sensor with a wavelength of 0.8 cm, whose measurements represent mainly the dry crust characteristics.

3.3 Photometric Characteristics of the Playas

Photometric measurements were taken at several locations on each playa, as shown on Maps A, B, C, and D. Whenever possible the photometric measurements (PH) were made simultaneously with measurements of surface, air, and under-surface temperatures (TE), hardness (HD), and moisture content (MC). The general

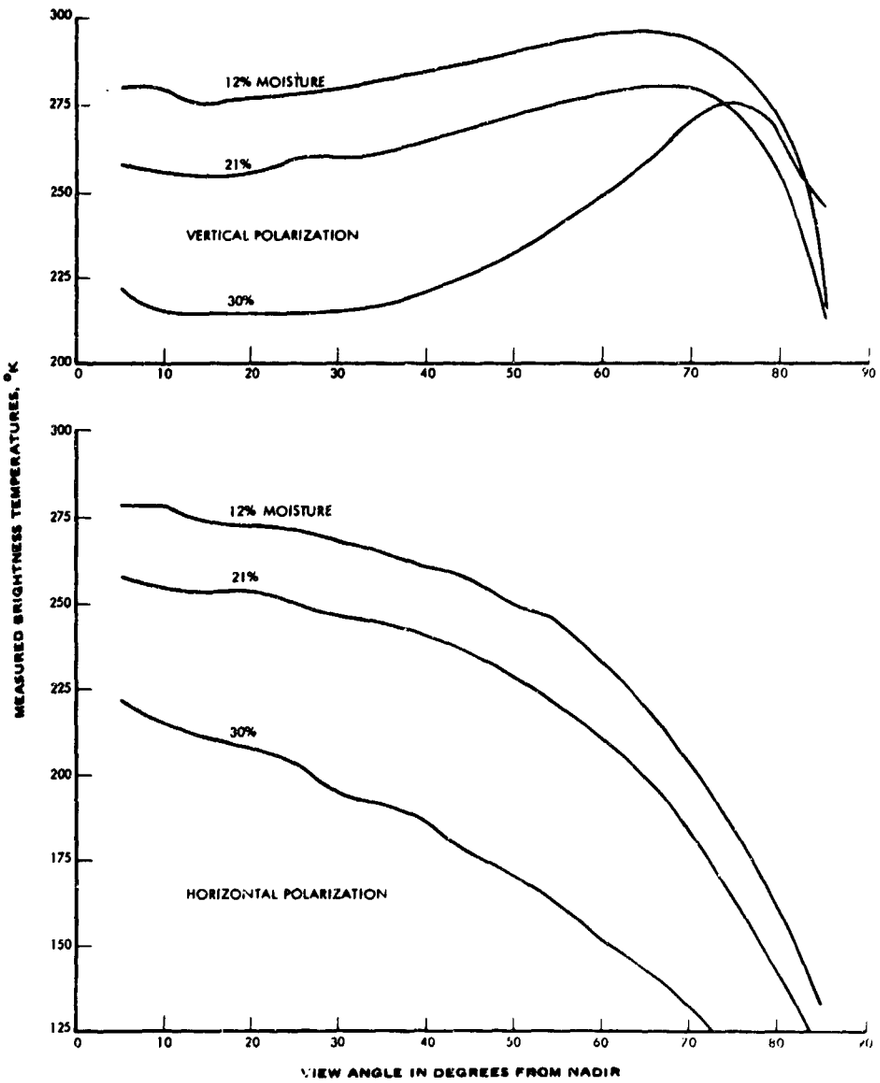

Figure 5. Radiometric Temperatures of Playa Sediments with Variable Moisture (λ = 2.2 cm)

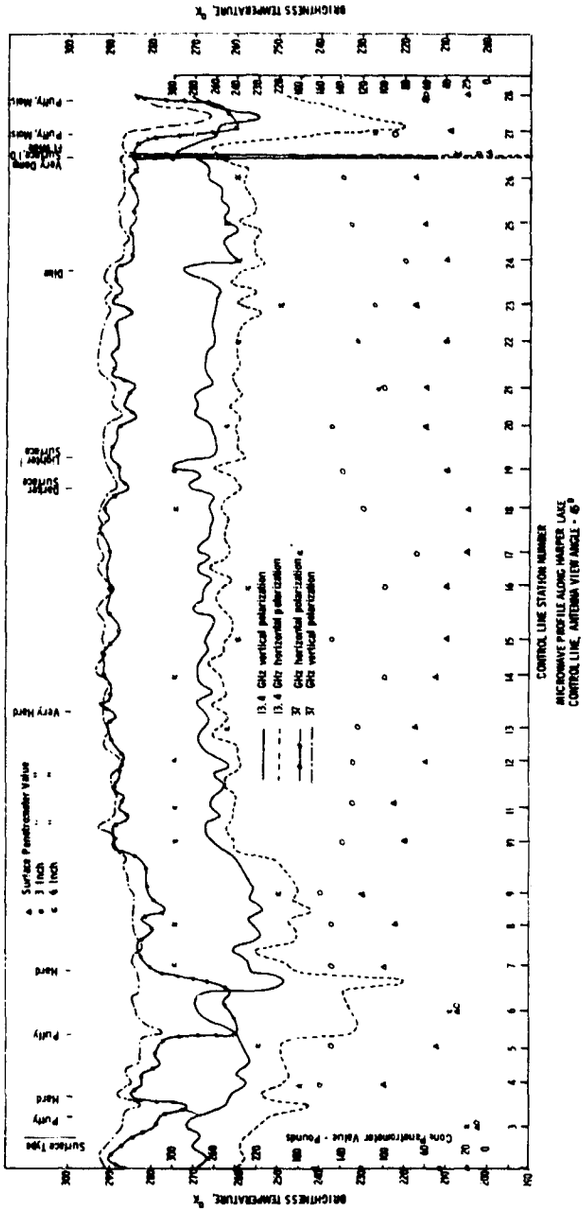

Figure 6. Microwave Provile, AFCRL Control Line, Harper Playa

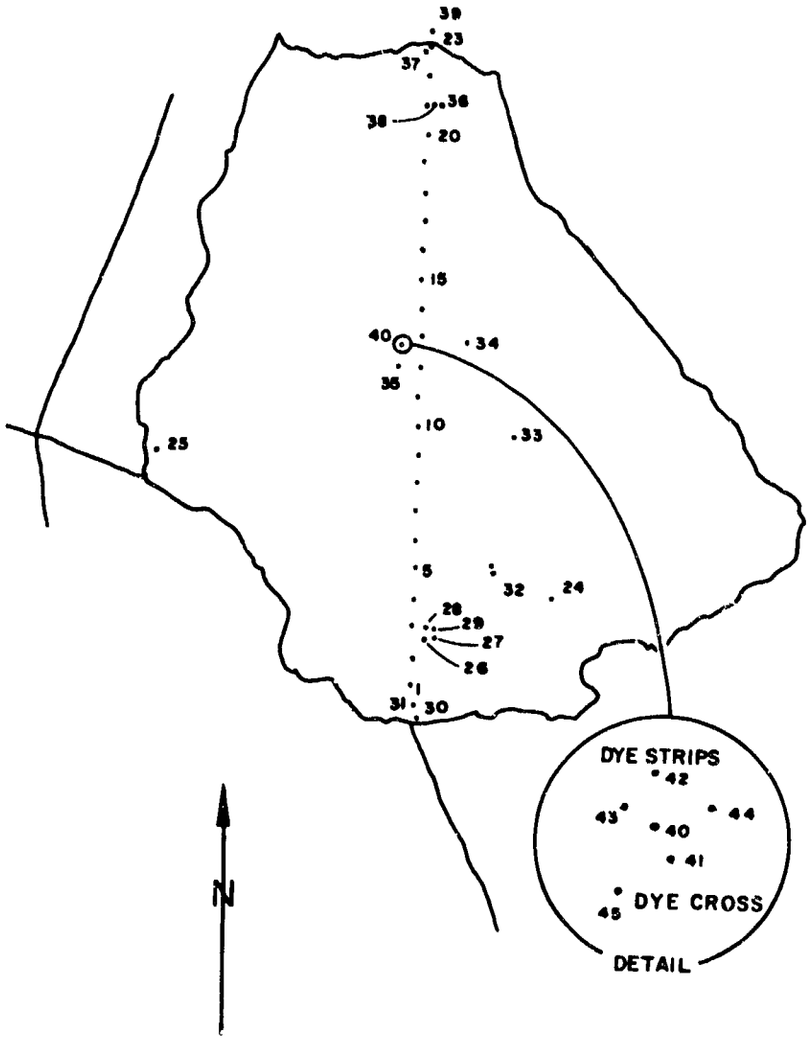

SCALE 1:62,500

Map A. Coyote Playa

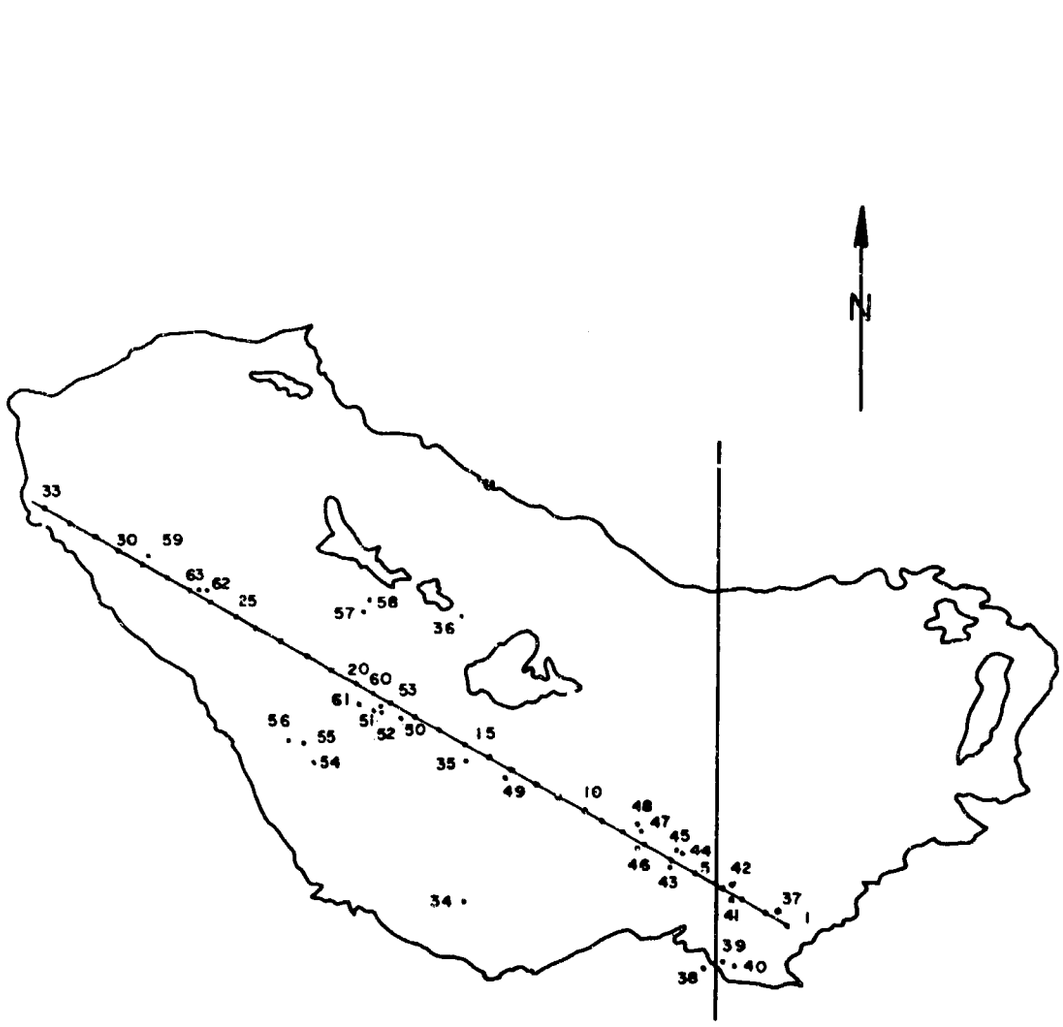

SCALE 1:50,000

Map B. Harper Playa

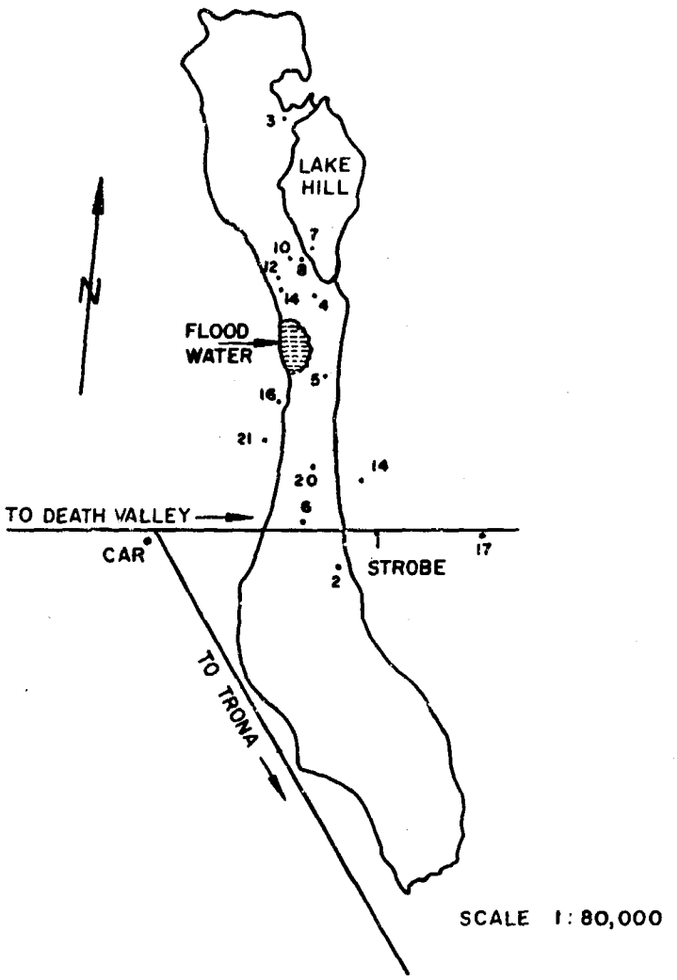

Map C. North Panamint Playa

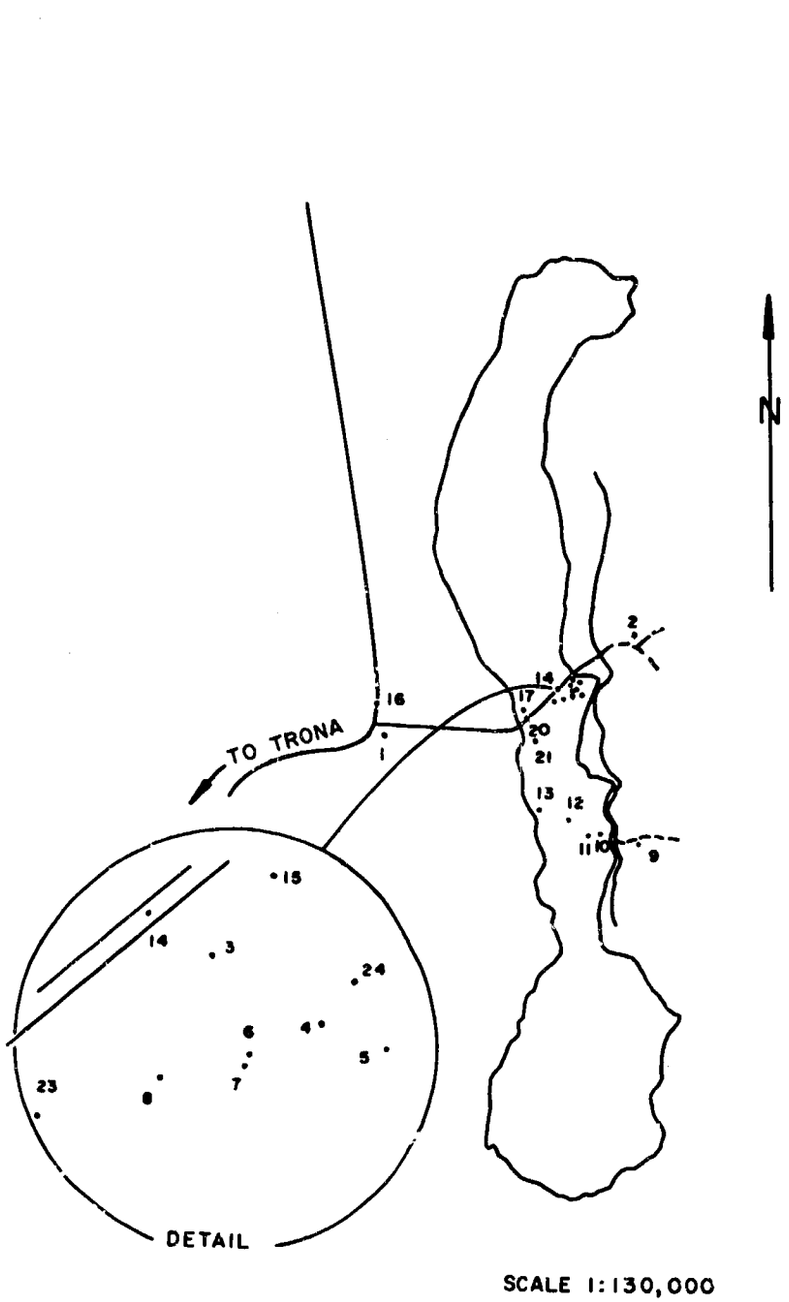

Map D. South Panamint Playa

appearance, condition, and composition of the ground surfaces were noted, as were the degree of cloud cover, wind velocity, and the local time. In addition, samples (SA) were collected for further laboratory reflectance study. Tables 2, 3, 4, and 5 show the various parameters obtained for each site.

The photometric measurements were made with a Spectra Pritchard photometer specially modified and equipped with all-quartz optics and glass filters (Cronin, 1967). The instrument was used in two modes: focused (Spencer, 1965) at infinity for distant objects with an aperture of 0.10°, and focused at near objects (3 to 5 m) with an aperture of 2.0°.

The transmission characteristics of the instrument without filters are shown in Figure 7. The transmission characteristics of the 10 filters used are shown in Figure 8. The luminance levels involved in obtaining the reflectance of the playa surfaces were quite large, so it was necessary to use a set of neutral density filters. The measured transmission characteristics of an ND3 filter, which was used most often, are shown in Figure 9. It is apparent from this figure that the defining relation for a neutral density filter ($D = -\log_{10} T$) must be used with caution if large errors are to be avoided. Whenever available the measured transmission characteristics should be used. Figure 10 shows the measured transmission characteristics of an HN38 linear polarization filter that was used at some locations to determine the degree of polarization of the reflected radiation in some wavebands.

The photometer was mounted on a heavy-duty tripod and securely tied down to a wooden platform that was constructed on the side of a carryall truck. By extending one of the tripod legs more than the other two, it was possible to cantilever the photometer beyond the edge of the platform and view the undisturbed surface directly below.

Figure 11 depicts a photometric and a moisture-content measurement in progress at one of the playas.

The detailed geometrical arrangement for the measurements is indicated in Figure 12, where S represents the source of radiation (sun), D represents the detector (instrument sensor), O is the center of the object (playa surface) whose luminance is measured, and Z is the local zenith direction. In most measurements the detector axis was along the zenith line. However, several measurements were made with varying instrument zenith angles. Insofar as playa surfaces are essentially diffuse reflectors, a normal view seems to be the most representative choice for characterizing them.

The instrument was calibrated in foot-lamberts. Since absolute luminance readings were not of direct interest—only ratios of luminance values were involved—the type of units used was not of consequence.

Table 2. Coyote Playa Sites

		HD	MC	PH	SA	TE
CP 1	First stake of baseline					
2	Second stake 0.2 miles N. of 1					
3		5				
5		13				
10		4				
15		3				
21	Brown flaky crust, wet appearance but dry	2	5	6A	1	6
22		1				
23	N. end on slope (gray rise)	11	7	16	26	7, T
24	Transitional ground 0.9 mile E of 4	9				
25	Damp, soft ground/dry ground					2A/B
26	Salt crust, 100 ft SE of No. 3	7A	4	11	4	4, T
27	Brown crust near salt stains, 150 ft SE of 3	7B	4A	12	2	4A, T
28	Salt top, 100 ft E of No. 3		10	4A		T
29	Brown flaky matter		10A	5A		T
30	S. end. Fan			9		T
31	Off S. edge. Hard salt crust	6	3	10	25	3, 3, T
32	Recent crack 0.5 mile E of No. 5 (in/out)			7, 8		T
33	Site of fire-baked area			13		T
34	Old crack. N-S, 600 ft E of 40, dry			6		T
35	Area of glazed surface, 100 ft S of 40			3, 4		T
36	Brown (hard) flaky crust, 100 ft E of 21	2	5	14	1	5, T
37	N. end of playa	10	6	15		6, T
38	Light dry-appearing surface 50 ft E of 21			7A	3	T
39	Off N. edge on sand (4-wheel drive needed)	12	8	17	24	8, T
40	Artesian well					
41	Dry water stain near 40			18		T
42	Dye strips 1/2, 1/1, 3/1		2	19, 20, 21		T
43	Near well. Wet/dry/H_2O	8A/8B	1	1/2		1A/1/2
44	Mud due to well water/ water stain	12A/12B		2A/3A 22, 23		43A, 43B T
45	Dye cross area		11	24, 8A		11, T

Table 3. Harper Playa Sites

		HD	MC	PH	SA	TE
HP 1	Stake No. 1	HD12				
3	Fire No. 1	HD15				
5		HD14				
6	Puffy ground	17				
7	Puffy ground	4				
9		HD 8				
11		HD11				
13	Fire No. 2, hard dry crust	7			20	7
15		HD 9				
18		21			10	
20		10				
21		24				17
23	Fire No. 3	HD20				16
25		23				15, N10
26		19				14
27		22				13
28	Puffy ground. Thin crust	18				12
29	Puffy brown crust	3		13	16	11
34	South strobe light					N5
35	Middle strobe light					N4
36	North strobe light					N11
37						N3
38	Fan. Playa edge near road	25A	1	1	22	1T
39	Playa crust near No. 38 (desert flat)	25B	2	2	21	2
40				1A		
41	Soft puffy ground	13	-	4	12	4, N1
42	Hard crust	16	3	3	15	3, N2
43	Soft puffy surface			5	14	
44		17	5	2A		5
45				3A		
46	Hard dry crust	4		6	11	6
47	Puffy edge, dark			4A		
	Puffy edge, light			5A		
49				7		
50	Stained puffy ground			6A	13	
51	Dark, 80 ft SW of No. 18			15		
52	Light-dark boundary			16	19	
53	Light. 50 ft SW of No. 18	21		14		18
54	Edge of salt tongue. White salt stain			10		8A
55	Self rising puffy crust near No. 56	6/26		9	18	9, N7
56	Salt stained wet puffy mud	5/27		8	17	8, N6
57	Playa-vegetation dune boundary	1		11		
58	Edge of dunes. White salt stain. Hard brown top	2		12		10
60	18 1/2	10				
61	Self rising crust/Moist area	28/29				
62	26 1/2A Near puffy ground					N8
63	26 1/2B Across from boundary to 62					N9

Table 4. North Panamint Playa Sites

STATION DESCRIPTION			HD	MC	PH	SA	TE
NP	1	Road-fan boundary. Strobe light					1
	2	Playa-fan boundary					2
	3	White playa surface					3
	4	Peeled area					4
	5	Crack 8-10 in. deep, N-S					5
	6	White playa surface					6
	7	Lake Hill photometer station					
	8	Fan. Dark. Near playa-fan boundary	8A		17,20	8	8A
	9	Playa. Hard. Light. Near NP8	8B		18,21	23	8B
	10	Playa. Near sandfinger		9A	22	6	9A
	11	Sandfinger. Near NP10		9B	23	7	9B
	12	Dark area	6	10	24		10A
	13	Light area. Near NP12	10		25	9	10B
	14	Mud curls	11		26,27	5	
	16	Alluvial wash			28,29		
	17	Photometer station by roadside					
	19	Gray matter			30		
	20	Light matter beyond NP19			31		
	21	To left of stream on fan			32		

Table 5. South Panamint Playa Sites

STATION		DESCRIPTION	HD	MC	PH	SA	TE
SP	1	Strobe light; off road junction					5
	2	Strobe light; off road on fan					19
	3	Self rising ground			1		3
	4	Light hard crust	2				
	5	Salt stained soft porous crust	1		5		16
	6	Light hard crust			2		
	7	Light hard crust			3		
	8	Self rising ground. Dark crust			4		
	9	Photometer station on road to mine					
	10	Light white area. E. edge of playa			33		
	11	White salt crusted area. Near SP10			34		
	12	Dark area (no salt top)			35		
	13	Light tan area			36		
	14	On road, 1.1 mile from W. edge					1
	15	Hard dry crust					15
	16	Road. Near Ballarat Monument					4
	17	Self rising ground near No. 20					7
	18	Automobile wheel rut (old). Near No. 20					8
	19	Fan. Near No. 20					9
	20	Road. Near W. edge of playa					10
	21	Salt silt crust, 0.35 mile from W. edge					11, 13
	22	Salt crust. Near No. 21					12
	23	Smooth, flat, salt-stained mud					14
	24	Smooth, salt-stained, flat mud					17

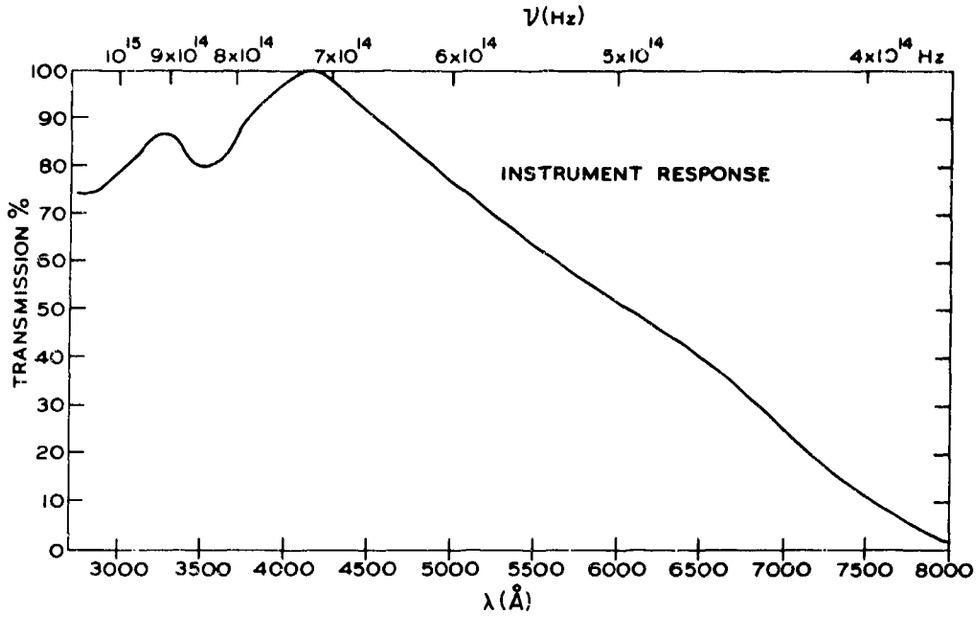

Figure 7. Transmission Characteristics of Photometer

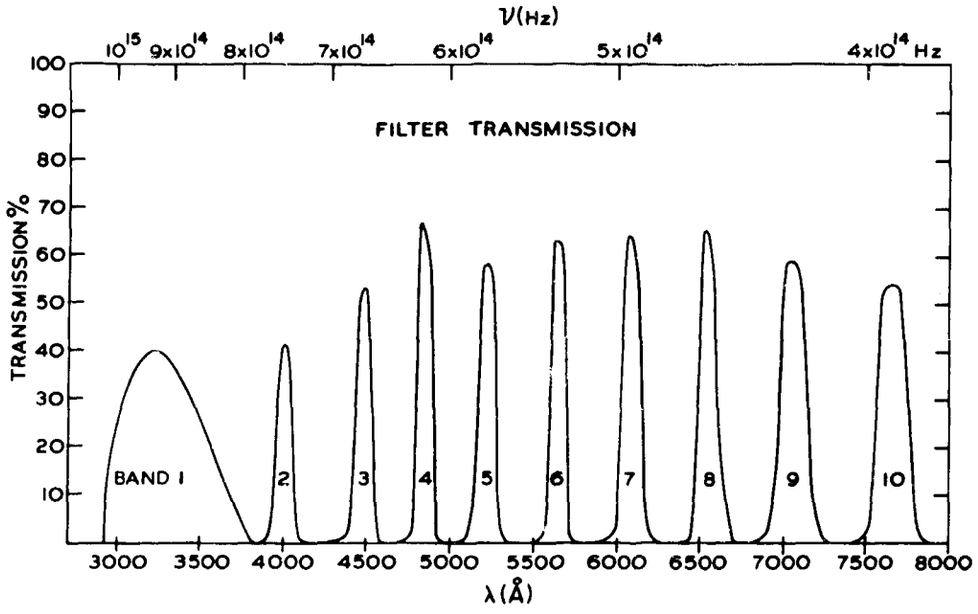

Figure 8. Transmission Characteristics of Spectral Filters

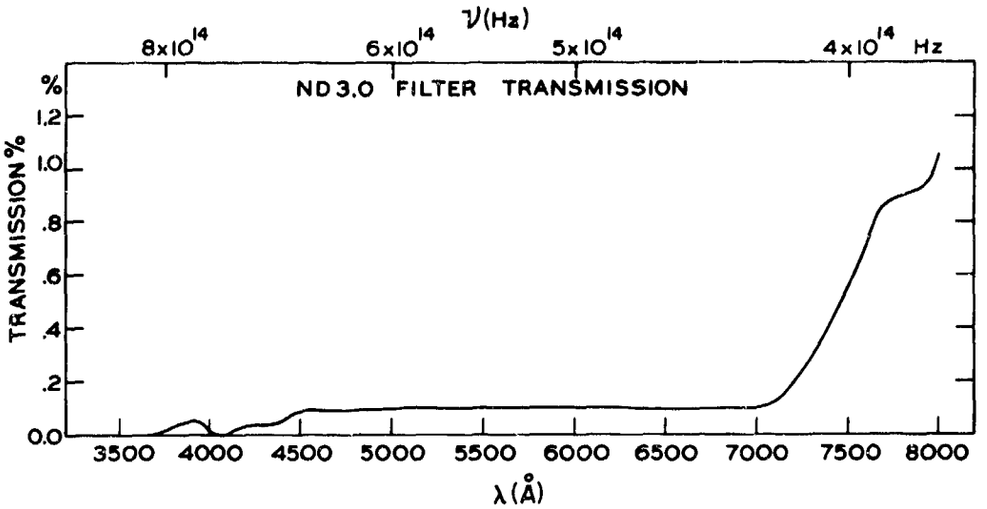

Figure 9. Transmission Characteristics of Neutral-Density Filters

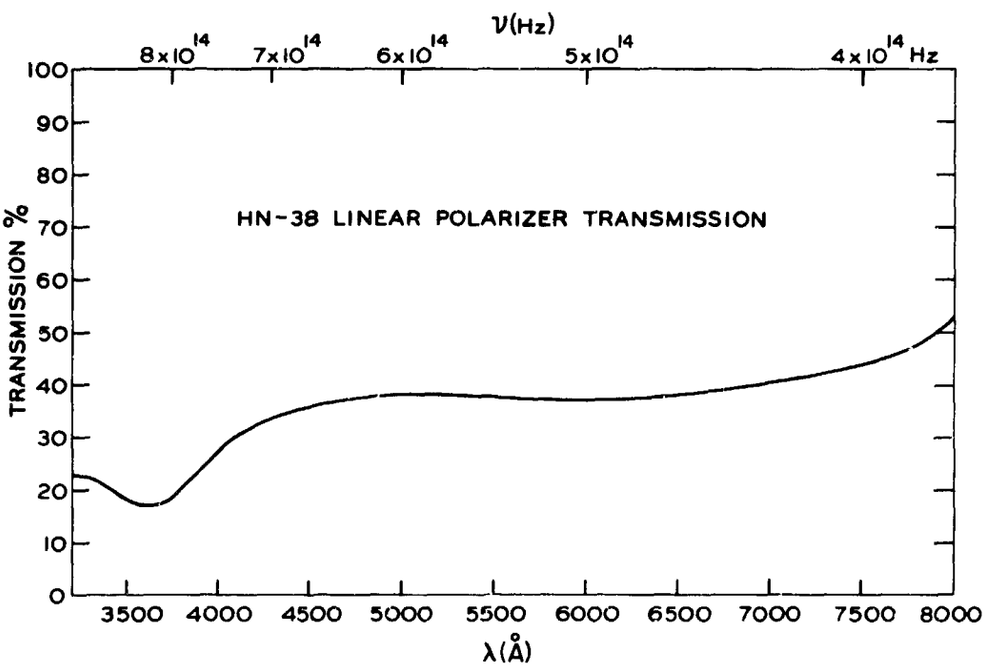

Figure 10. Transmission Characteristics of Polarization Filters

Figure 11. Field Measurement Operations

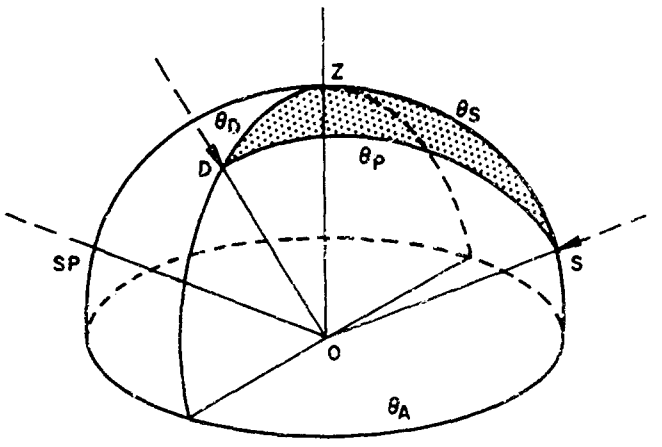

SOZ	PLANE OF INCIDENCE
DOZ	PLANE OF MEASUREMENT
SOD	PLANE OF SCATTERING
SP	SPECULAR POINT
θ_S	SOURCE ZENITH ANGLE
θ_D	DETECTOR ZENITH ANGLE
θ_P	PHASE ANGLE (SCATTERING ANGLE SUPPLEMENT)
θ_A	RELATIVE AZIMUTH, (POSITIVE CCW FROM SUN)

Figure 12. Geometry for Reflectance Measurement

Some representative raw data as recorded in the field appear in Appendix A, and are referred to in the text by designations such as CP43A (for Coyote playa sample No. 43), etc.

The reflectance of natural surfaces exhibits a rather complex dependence on the wavelength, polarization, and angle of incidence of the incident radiation as well as on the viewing angle and the nature of the surface under investigation. Furthermore, to the extent that a natural surface absorbs the incoming radiation, optical path reversibility cannot be guaranteed. These facts make the characterization of such a surface by means of one or two parameters of limited value. It appears, therefore, that as the complexity of a surface increases the number of parameters needed for adequate characterization increases.

Krinov (1947) classified natural surfaces in four broad categories according to their average reflectance values. Representative materials and reflectances for the four classes are: type 1, dry black soil (3 percent); type 2, dry silt (10 percent); type 3, saline soil (20 percent); and type 4, clay (60 percent). Krinov's measurements indicate a monotonic increase in reflectance with increasing wavelength for these natural surfaces in the visible region. In contrast, the reflectance of vegetation exhibits minima in the blue and red bands and large increases in the near IR. Ashburn and Weldon (1956) studied the reflectance properties of several areas in the Mojave Desert and showed that the variation of diffuse reflectance with angle of incidence exhibits a maximum in the vicinity of 75°. This reflectance maximum becomes more pronounced with increasing wavelength. Several other investigators studied the reflectance of complex and/or natural surfaces, mostly oriented toward interpreting the reflectance characteristics of the moon.

Hapke and Van Horn (1963) made extensive experimental comparisons of the reflectance properties of special complex surfaces with those of the moon. Hapke (1963) derived a theoretical expression for the photometric function of the lunar surface that very nearly duplicates the measured lunar data. Coulson et al (1965) studied the reflectance of natural surfaces, including polarization considerations. These measurements were detailed enough to permit construction of bidirectional reflectance maps at two wavelengths for red clay and white quartz beach sand.

The playas studied represented a great variety of soil surfaces. Figure 13 is a photograph of samples collected at the locations identified on the maps. In general, the presence of a salt crust is responsible for increased reflectance over that of the adjacent brown flaky crust, but this is not true at all wavelengths. An example of this is that reflectance values of CP27 in bands 7, 8, and 9 are higher than those of CP26. The presence of moisture, which is of primary importance in trafficability considerations, resulted in a marked decrease of the reflectance of the playa surfaces. This dramatic reflectance reduction is due to the fact that water has a much smaller albedo than that of the materials involved. Along with

Figure 13. Playa Soil Samples

this reduction in reflectance there is an increase in the polarization of the reflected radiation with increasing wetness (CP43A, CP43B, CP43A1, CP43B, and CP44A, CP44B). In the visible region, which was roughly covered by the 10 bands of the spectrophotometer, there is almost no spectral structure other than the general increase of reflectance with wavelength. In view of this fact, one would expect that the spectral structure of the reflected radiation from wet surfaces would be completely obliterated.

Those wet-appearing surfaces that are in fact dry (NP14A, NP14B) at large observation angles, θ_D, could, under certain conditions, be distinguished from areas that are actually wet by the presence or absence of spectral structure. This, however, is not a unique requirement as the surface need not be wet. Such a surface, when viewed from a different angle, in particular near $\theta_D = 0^\circ$, will not appear wet, and, furthermore, the reflectance values will be higher than those for a wet surface. A third possible criterion for this differentiation is the degree of polarization of the reflected light. Since the amount of specular reflection is small (for most playa surfaces), the degree of polarization is normally small; since light reflected from a wet surface displays a rather high degree of polarization, a small degree of polarization indicates a low moisture content.

Measurements of polarization should, preferably, satisfy the condition $\theta_S + \theta_D = \pi/2$ (detector 90° from the sun), because this is the position of maximum polarization. On the other hand, one must avoid the three neutral polarization points (Sekera, 1957). The locations of the neutral points are strongly affected by the aerosol concentration and the atmospheric turbidity, but they are insensitive to the changes of the diffuse reflectance of the ground surface. Since the neutral polarization points are situated in the plane of incidence, one way to avoid them would be to make the measurements in the plane normal to the incident direction. Under overcast conditions, these criteria would not be applicable due to the large proportion of indirect radiation. The scattered sky radiation is polarized and the dependence of reflectance for scattered radiation on its state of polarization is quite strong. However, as observed by Kondratyev (1965), in the case of total radiation the polarization of the scattered radiation of a cloud-free sky has almost no effect on the albedo of the underlying surface. Since the playas are located in relatively arid regions, this limitation is not too severe.

The roughness of the surfaces plays a major role in both the total and the spectral reflectance. Almost all natural surfaces reflect radiation in a non-lambertian way. In the case of the playas, an increase in surface roughness (as determined visually) resulted in a decrease of reflectance. This reduction in reflectance is most probably due to the greater absorption of radiation by the "cavities" in the rough surface as compared to a smooth lambertian surface. This observation is in agreement with Hapke and VanHorn who studied several

artificially produced "rough" surfaces in which the interconnected voids were of major importance. Playa surfaces are not characterized by extensive interconnected voids, in general, but certain conditions of "self-rising" ground exhibit some features of this nature. The presence of strong backscattered radiation, which is an important feature in the reflectance of lunar-like surfaces (Coulson et al, 1965; Hapke et al, 1963), was not observed in detail due to the lack of the special instrumentation set-up needed for such measurements. An indication that such strong backscatter does indeed take place may be inferred from the data on SP3 and HP55.

The composition of the materials present in the surfaces was largely clay or silty clay. In some instances when the measurement was outside the lakebed the soil contained some sandy elements. In the case of particles precipitated in calm water, their shape and preferred orientation significantly affect the reflectance of the surface for a period after the disappearance of free water. As the surface is weathered, however, the mode of settling is disturbed and the orientation distribution is randomized. Thus, initially, some clays may settle out parallel to their prominent cleavage, resulting in increased specular properties (Cronin, et al, 1968). However, after weathering, the specular properties are reduced or obliterated. It may, therefore, be stated that a specular appearance on a playa surface is a recently sedimented surface.

In areas where the surroundings are dominated by soil and rock surfaces there is an enhancement of the longer wavelengths due to the increasing reflectance of these materials with wavelength. This effect, previously noted by Ashburn and Welden (1956), Coulson (1966), and others, is most pronounced at low sun angles when the shorter wavelengths are attenuated by Rayleigh scattering.

In certain areas of the playas there are cracks (Neal, 1968), some of which are 0.30 to 0.5 m wide and several times as deep. These constitute an obvious hazard to trafficability. Photometric results indicate that the interior surfaces of cracks have a much lower reflectance than the surrounding areas (CP32A, CP32B, CP34). The percentage of area covered by cracks is small, so their effect on the radiation received by aircraft sensors is likely to be small or undetectable. Their presence was not ascertained by radiometric techniques; however, in the case of straight line (or circular) cracks, the techniques of optical data processing (Mitchel, 1969) show promise for use.

3.4 Photography and Imagery Interpretation

Remote detection and evaluation of soil properties and moisture conditions of the playas depend primarily on reflectance changes. In general, the albedo or reflectance of desert soils varies with the wavelength of the incident radiation. Such spectral reflectance variation makes the use of spectrophotography

particularly useful, as will be evident in the later examples. For dry clays, maximum contrast in the visible spectrum occurs within the 650 nm to 850 nm range. In this wavelength region water absorbs greater amounts of the incoming radiation, so that water-covered or moist surfaces are usually distinguishable from dry clay material.

The predominant color of playa soils is characteristically light brown on a dry surface; below the surface they become darker brown with increasing moisture. Where salt incrustations occur, the color is white to brownish gray, depending on the amount of salt. At the dry-clay areas, the characteristic color is light tan. Color and color-infrared photography are, therefore, very useful in distinguishing salt-covered or dry-clay surfaces; black-and-white photographs of these surfaces often show nearly identical gray tones.

Infrared imagery of playas, particularly that taken at night and compared to daytime infrared imagery, enables surficial soil variations to be distinguished. This is due to soil density and moisture differences that influence the heat capacity and emissivity of the soils and their ensuing radiometric response, as shown in their thermal patterns on the imagery.

The main objective of the remote-sensing investigation was to evaluate the playa conditions affecting trafficability. Interpretation of the photography and imagery is, therefore, made to indicate factors such as soil moisture and density, irrespective of the particular playa involved. Selected examples of these interpretations follow.

3.4.1 Moisture Conditions

Figure 14, a black-and-white vertical aerial photograph of Harper playa, shows the prevailing moist areas at its south edge as obvious darker tones. A closer view of these moist areas, shown at the bottom of Figure 15, reveals the noticeable tonal differences corresponding to amounts of moisture and vehicle ruts that have churned up the surface and penetrated to softer moist areas. These show obvious wet spots as dark tones and similar streaks of moist "fingers" extending into the dry playa that has light tones even on the black-and-white photograph.

The advantages of spectrophotography for enhancing the appearance of soil moisture are evident in Figure 16, a composite of four narrow-band photographs of the area outlined in Figure 15. Bands 2, 4, 6, and 7 were selected from the nine bands for contrast. The superior enhancement of the moist areas in Band 6 is marked, inasmuch as the reflectance contrast of the wet and dry playa soil is greatest in this particular spectral region. The elimination of much of the atmospheric haze at this wavelength peak (650 nm) could add to this enhancement.

Figure 17 shows a surface view of the terminus of the largest moist "finger." The salt scum on the surface might be misleading as to the existence of moist soil, but the aerial photography reveals the moisture easily.

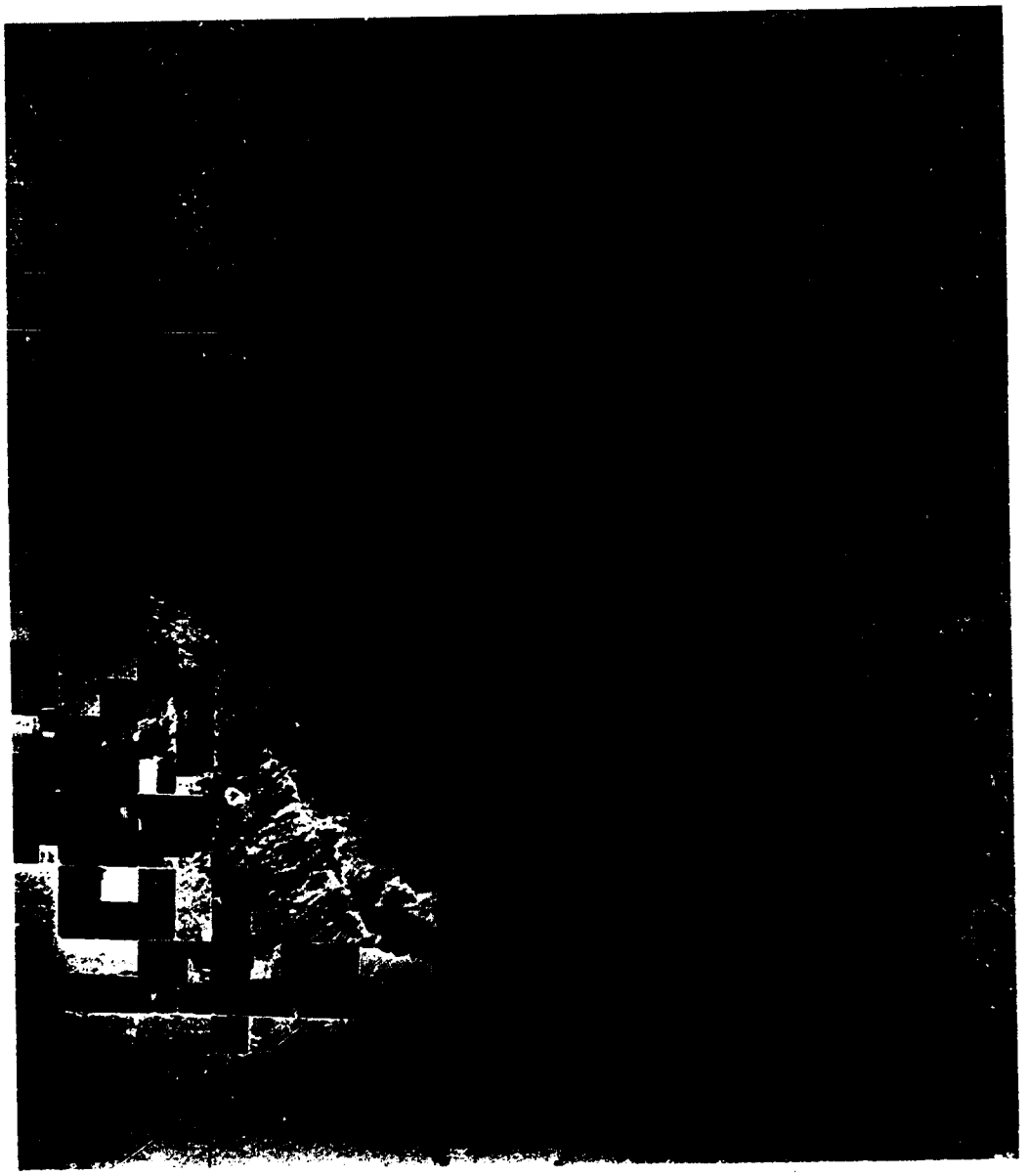

Figure 14. Vertical Aerial Photograph of Harper Playa

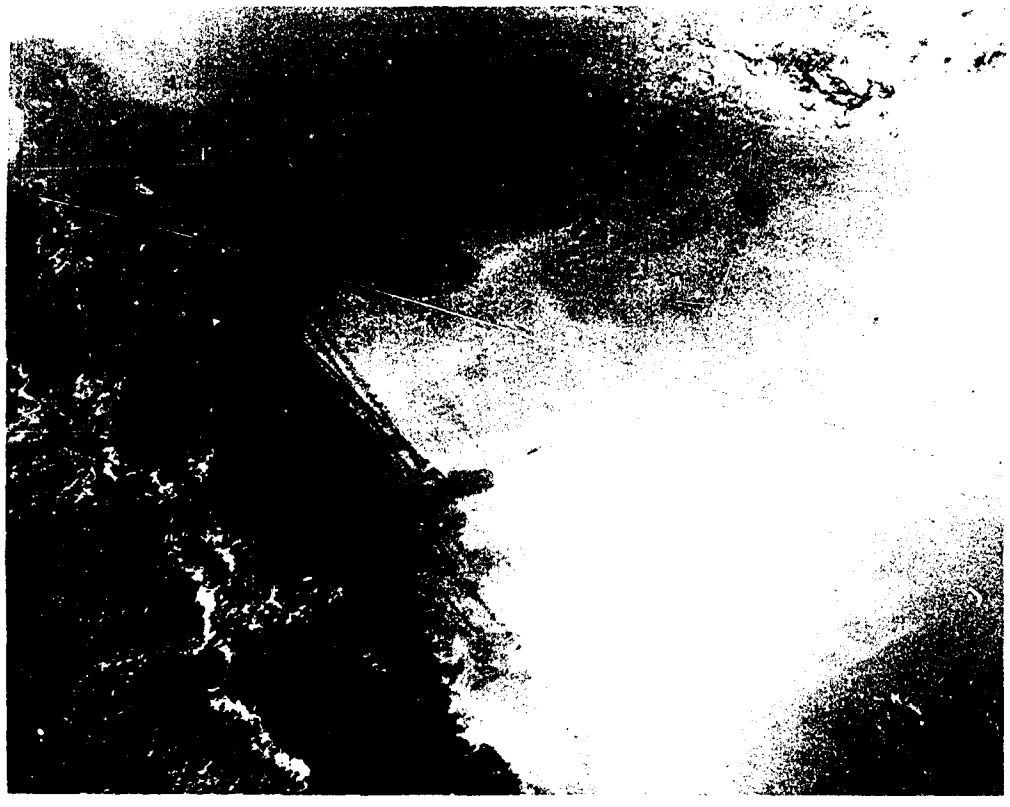

Figure 15. Aerial Photo of Wet Playa Area (Harper)

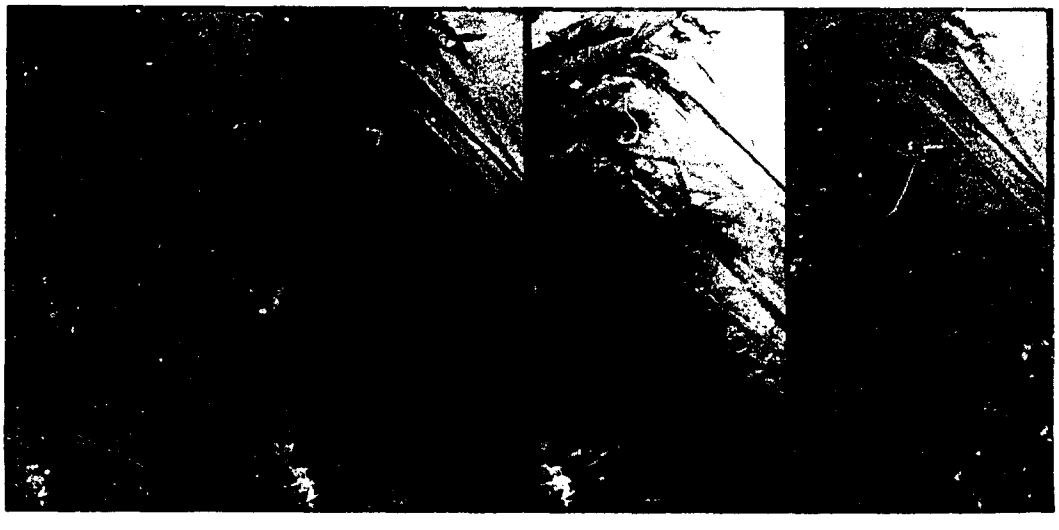

Figure 16. Composite Spectrophotograph of Moist Area (HP61)

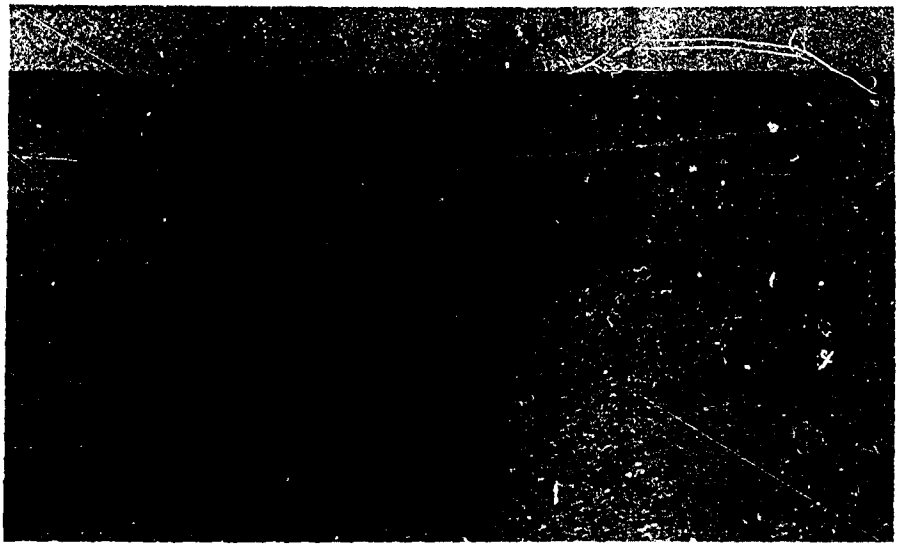

Figure 17. Surface View of Moisture Finger (Location HP54, HP55)

Color (taken through a yellow haze-cutting filter) and color infrared photographs of the same area revealed through color changes, which were apparent on the original photographs, that the moist areas were definitely wet.

Infrared imagery taken of the same portion of the playa also enables detection of moisture anomalies. Figures 18 and 19 are infrared imagery taken during the day and night respectively. The moist fingers are more defined in the daytime imagery than at night, due to the temperature reversal of the moist areas previously cited. The standing water and moist playa clays at the left end of the nighttime imagery, as well as the large spots of soft friable surface in the right center of the imagery, show as dark areas, as compared with the light tones of the hard dry clay crusts. The reverse tonal appearance is noticeable in the daytime imagery, wherein the dry areas show as dark tones for most of the playa at the top of the imagery, and the softer moist spots are light tones.

The result of flooding of playa surfaces is often the formation of a hard crust. In some soil types this may result in the generation of mud cracks and a polygonal structure of the surface. Such a formation is found at the west end of North Panamint playa, resulting from an outwash from the nearby mountains. These large polygons have a thin platy veneer surface that is readily identifiable on aerial photographs, as is shown on the bottom of all the photographs of Figure 20, another composite of four multispectral photos. Bands 1, 4, 6, and 8 were chosen for contrast. Again the contrast is most evident in Band 6, which also emphasizes the vehicle ruts across alternately wet and dry soil spots seen just above the large polygonal structures.

Figure 18. Night Infrared Imagery of Harper Playa

Figure 19. Day Infrared Imagery of Harper Playa

3.4.2 Soil Density

A soft, dry, puffy surface is commonly found on many of the dry lakebeds, particularly at the east end of Harper playa. This may also be accompanied by salt stains and a thin salt crust surface. Another look at Figures 18 and 19 also indicates the soil-density-discrimination capability of aerial infrared imagery (Neal, 1968). The nighttime imagery of the soft puffy areas shows them as dark tones, resulting from their lower density and hence less heat capacity than the hard dry crusts. In the corresponding daytime imagery the soft areas appear warmer and hence show as light tones. The salt content of such crusts also contributes to different emissivity values and ensuing temperature reversals.

Figures 21 and 22 are composites of four multispectral photographs showing typical puffy ground areas. Again Bands 4 and 6 enhance the tonal contrast between the puffy and hard ground. Analysis of color and color-infrared photos shows no marked advantage of using these emulsions over multispectral or black-and-white film for differentiating soil-density conditions.

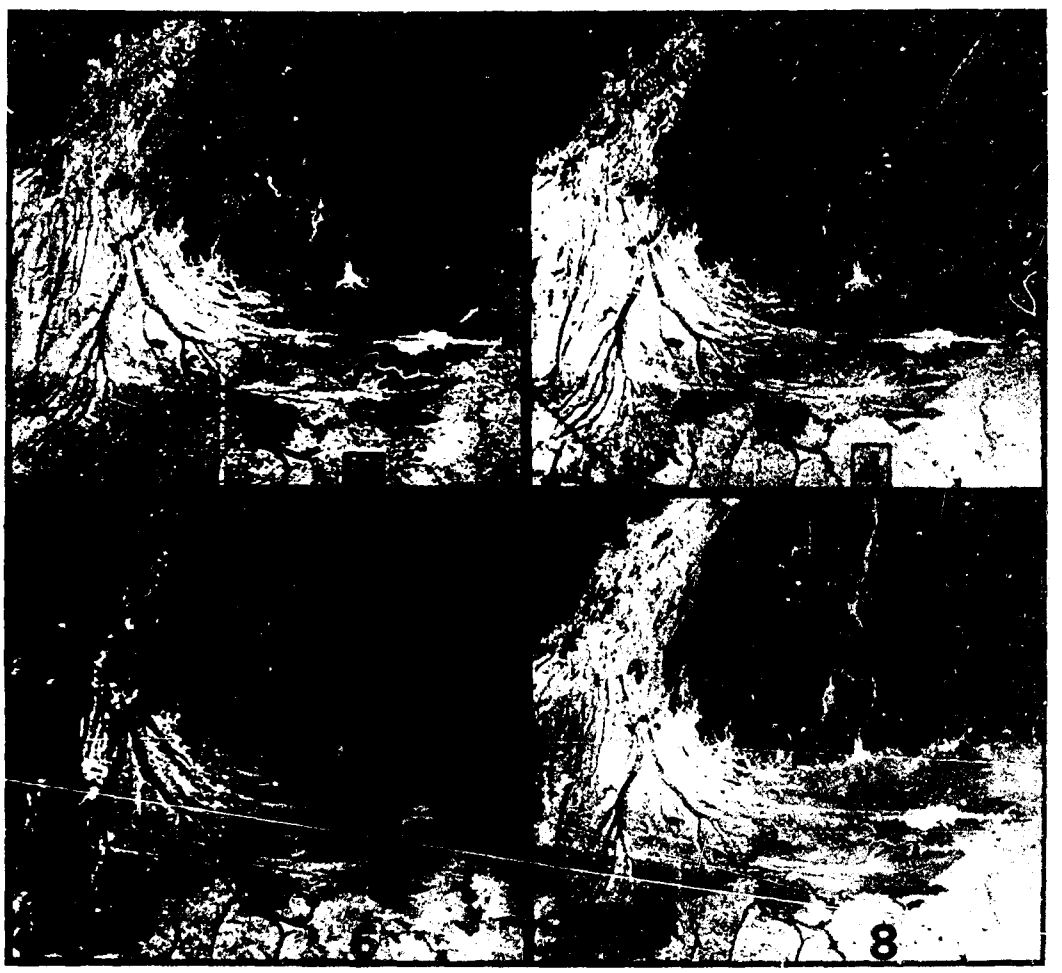

Figure 20. Composite Spectrophotograph of Platy Ground Area (Location Near NP14)

Figure 21. **Composite Spectrophotograph** of Puffy Ground (Location HP41)

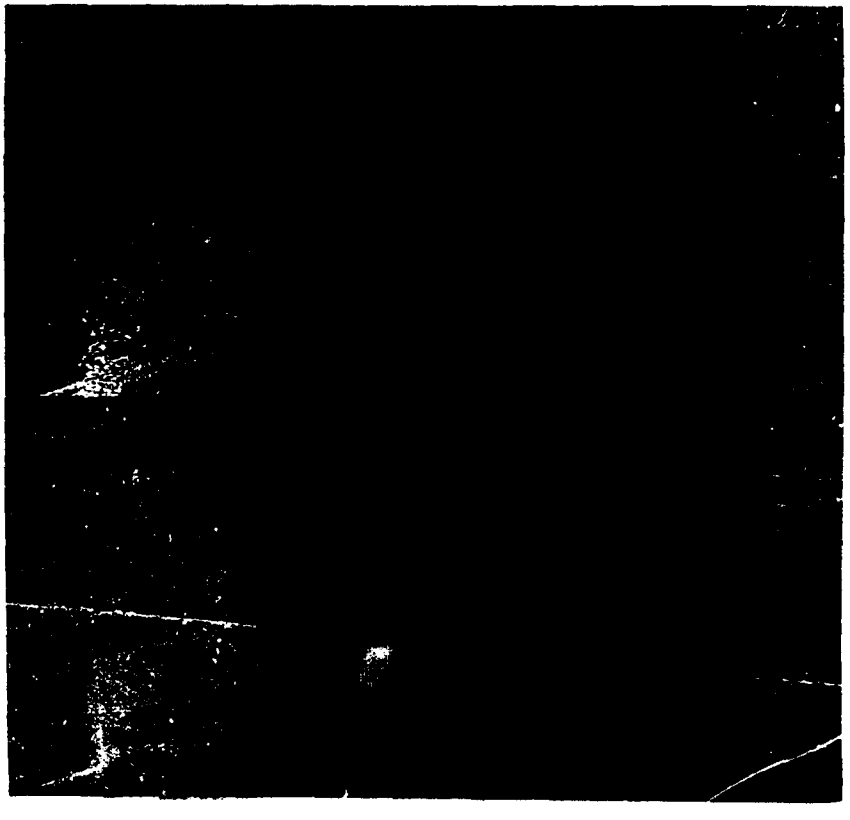

Figure 22. Composite Spectrophotograph of Puffy Ground (Location HP47)

The North Panamint area in particular exhibits large polygonal crack and platy structures, noticeable at the west (right) side of Figure 23, a black-and-white vertical photograph. This is a large fan-shaped deposit that extends out from the wash on the western slopes. It is material that was washed down during a recent flood; although fine-grained silt in nature, it is not the fine-grained lacustrine material of the sediments of former Lake Panamint of the Pleistocene age.

The deposit as shown in a ground view (Figure 24) was examined photometrically from a distance, because its different appearance at varying aspect angles might be misconstrued as revealing moisture. At ground level, the shadows produced by the upturned mud platelets cause a decided variance in reflectance. On the ground much of this area is actually lighter in tone, because a scum or alkaline coating on the dried platelets has a higher reflectivity than the adjacent zones. Figure 25 shows a ground view of this formation.

Such a feature, produced by outwash, is common on playas as it is concentrated at the terminus of a principal drainage channel. The problem insofar as trafficability is concerned is to determine if the area is moist or dry. Figure 26, a composite spectrophotograph, shows a similar formation at Coyote playa, but the Coyote area was moist. The dry condition at North Panamint could also be potentially hazardous for mobility, as the dry large platelets are brick-like in size and weight and could damage an aircraft when thrown up by the landing gear.

Adjacent to the northern periphery of the drainage fan at North Panamint is an area of darker-colored sediment that appears as though it could be moist. This darkening is prominent on the color photography and on the spectrophotograph shown as Figure 20, which is the outlined area of Figure 23. It is a stained zone resulting from rearrangement of the surface sediments during flooding, probably at the same time the drainage fan was formed. Conventional, color, color-infrared, and multispectral photography all can reveal both the fan and the stain, but cannot discriminate between them; the infrared imagery can.

Figure 27 shows night (top) and day infrared imagery of the playa. While the nighttime imagery does not show a difference in these areas due to their similar heat capacity, the daytime imagery can discriminate both. The white zone adjacent to the drainage fan is the stained area. The black central zone in the stained area is comparable to the area in the fan. If the area were moist, it would have registered as a dark tone.

4. VISUAL INDICATORS OF SOIL MOISTURE

Since the moisture content of a bare soil surface greatly affects its strength, slipperiness, and stickiness, any means of estimating or indicating this moisture

Figure 23. Aerial Photograph of Polygonal Soil (Location NP5)

Figure 24. Surface View of Polygonal Soil Area (Location near NP5)

Figure 25. Surface View of Platy Polygonal Material (NP14)

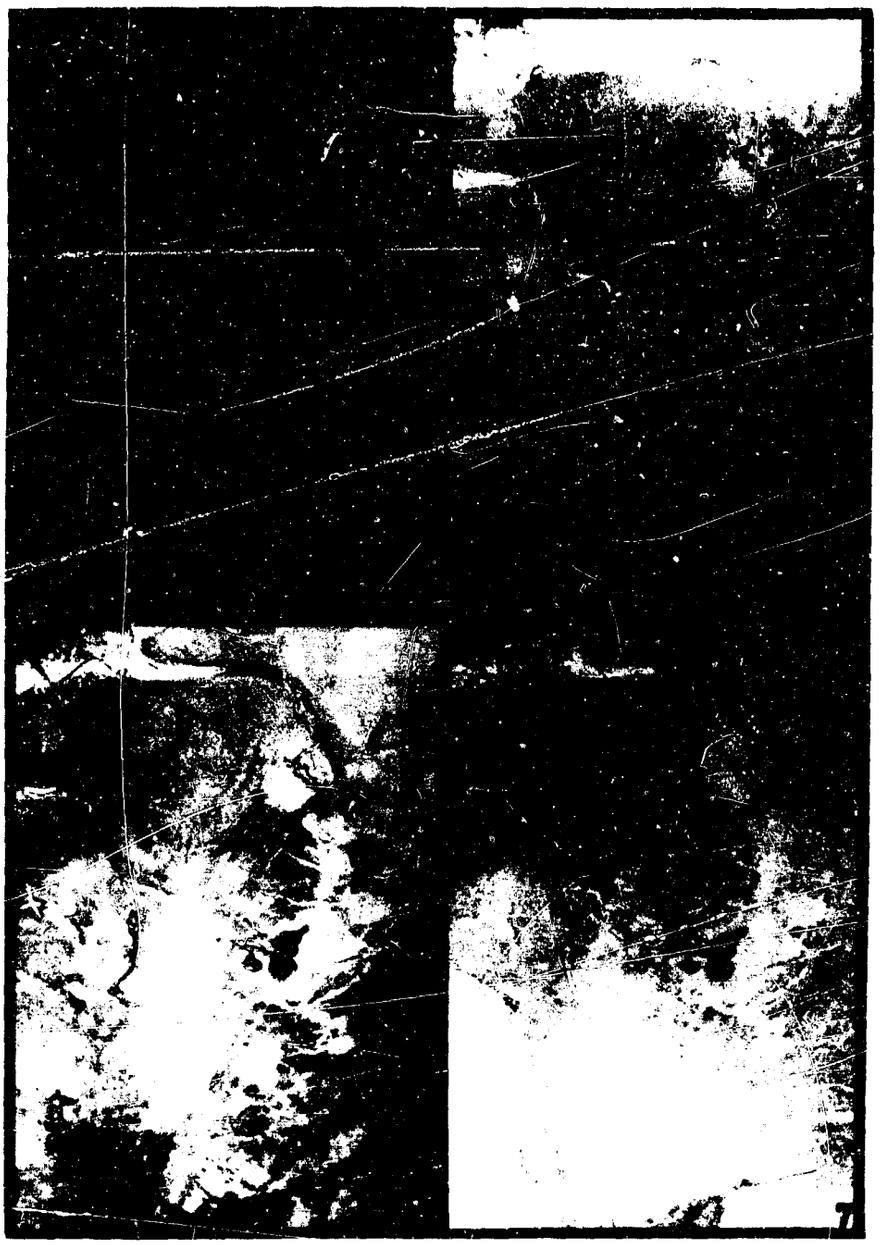

Figure 26. Composite Spectrophotograph of Moist Platy Area (Coyote)

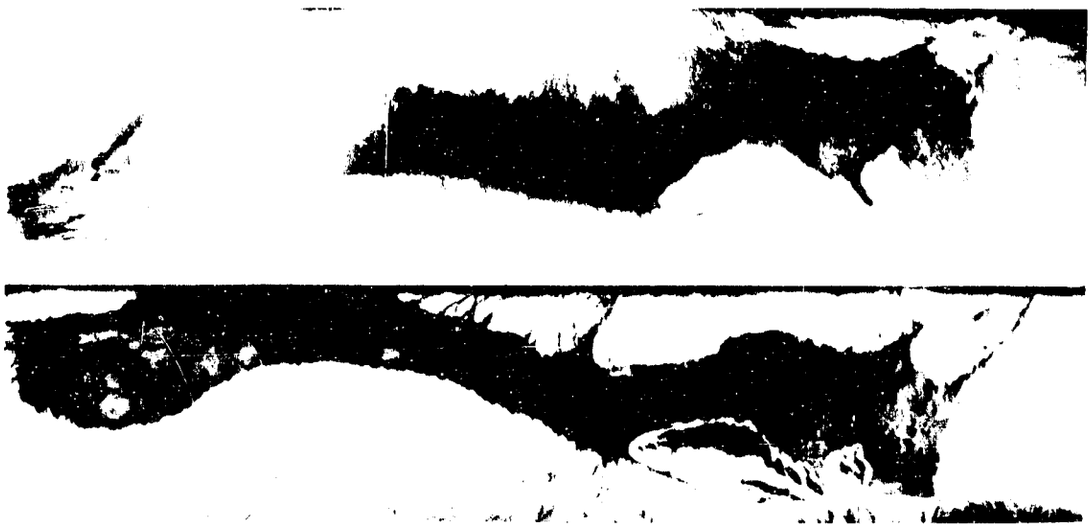

Figure 27. Night and Day Infrared Imagery of North Panamint Playa

content or its temporal changes will be of value in monitoring such remote site operational capability.

An experiment to determine the suitability of moisture-sensitive dyes as indicators of the presence of soil moisture was undertaken at Coyote playa. Cobaltous chloride ($Co\ Cl_2 \cdot 6\ H_2O$), a chemical that is pink in its hydrous (wet) state and turns blue when anhydrous (dry), was used. Solutions of this chemical dye were sprayed on test strips of the playa surface in 1:1, 1:2, and 1:3 concentrations. Moisture content of the playa surface was measured at intervals during the drying cycle with a "Speedy" moisture tester in standard units of percent moisture by weight. Soil temperature and air temperature were measured at the same intervals.

The initial moisture content of the dry playa surface was 3.4 percent and that of the adjacent wetted area was 28.8 percent. At the time of the experiment the dry soil temperature was $68^{\circ}F$ and the wet soil temperature was $72^{\circ}F$; air temperature was $95^{\circ}F$. The color of the previously dry test strips after dye application was a light brown, changing to the expected blue within less than 1 hr. At the time the color change became strongly evident, the moisture content of the test strips was 15.6 percent and the soil surface temperature was $86^{\circ}F$. The photograph in Figure 28 indicates the appearance of the strips, with little effect noted of varying dye concentrations.

The strips were left intact during the night; upon inspection early the following morning it was found that the deposition of moisture and the humidity of the air had

Figure 28. Surface View of Dye Test Strips (CP42)

caused a reversal of color back to the pink state. However, with increasing air temperature the surface soon changed color to the blue state, indicating its obvious dryness and demonstrating the reversibility of the process.

To demonstrate the usability of such indicators for airborne monitoring, a large cross-shaped playa area, with each leg 10 ft wide and 80 ft long, was sprayed with a 1:3 dye concentration that would be visible from the aircraft taking photography and infrared imagery. Initial dry and wet soil temperatures were 68°F and 72°F respectively. The blue color of the treated area soon became evident. The surface moisture content of the sprayed area at the time of the aerial photography 1 hr later was 3.8 percent, with soil temperature 86°F. One leg of the cross was kept wet as a contrast control. Figure 29 shows the appearance of this area at that time.

Ground photography and photometric measurements of the surface reflectivity were taken through narrow-band filters that duplicated those used in the aerial multispectral camera.

The presence of an artesian well at the midpoint of Coyote playa enabled the generation of a large wet soil area 175 ft in length whose darker-brown color contrasted well with the normal dry playa surface. The dye test areas were immediately adjacent to this wet area.

Figure 29. Surface View of Dye Cross Area (CP45)

The airborne photography, taken at 10,000 ft above Coyote playa, shows the obvious wet area and the experimental dye-marked area in good contrast to the surrounding dry playa surface. An aerial color-infrared photo, not reproduced here, revealed the tonal differences of the dye cross and the leg of the cross that was kept wet as the control. Black-and-white aerial photos also show the obvious moisture differences of the test areas.

The "multiband" aerial photography especially indicates the differing reflectance of the playa and test areas appearing in the narrow-band filtered photography. The best contrast and appearance of the dye cross area was found in Band 6, which peaks at 650 nm in the visible region of the optical spectrum, as is shown in Figure 30.

The experimental arrangement for investigating the reflectance properties of the dyes was similar to that for other playa locations. Comparison of CP42A (purple surface, freshly sprayed) with CP43A (wet area near well) and CP43B (dry area near well) reveals a marked difference in reflectance in the short wavelengths. Thus in Bands 1 and 2, CP42A is almost one order of magnitude more reflective (in the zenith direction) than either the wet or the dry surface adjacent to it. These reflectance differences become smaller at the longer wavelengths. There is almost total absence of polarization in the light reflected by the dye patterns. As the concentration of dye is decreased, the reflectance and polarization tend towards those of undyed surfaces of similar composition.

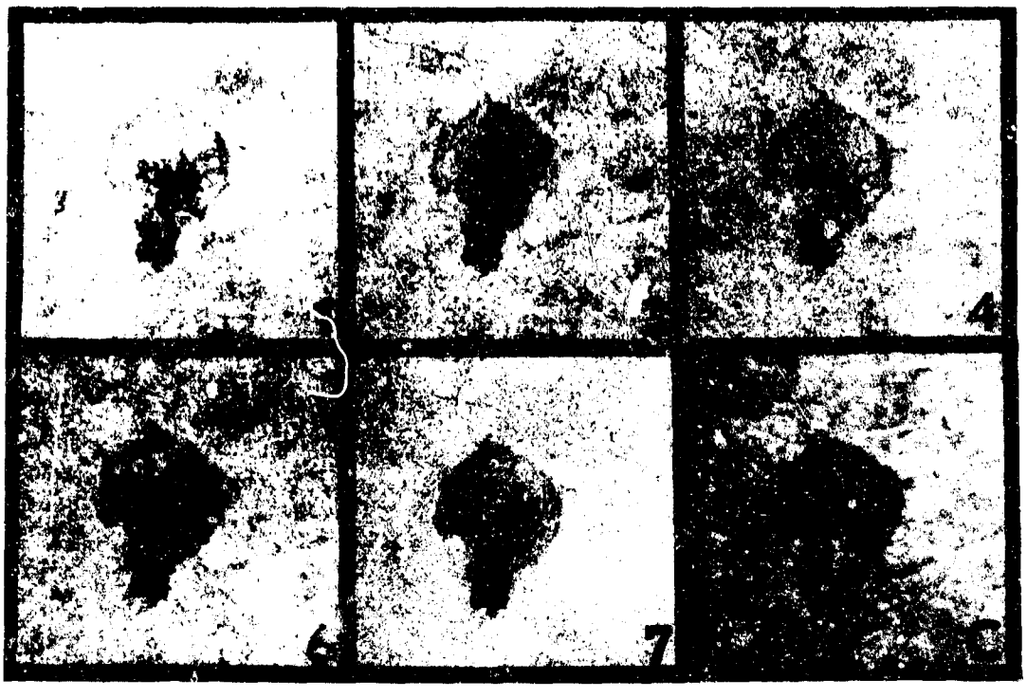

Figure 30. Composite Spectrophotograph of Dye Cross Area (CP40-CP45)

5. CONCLUSIONS

Conclusions from the dye experiment are that dye application is a feasible method for indicating the lack or presence of surface moisture and that the indications are readily visible from medium-altitude aerial photography. The optimum reflectance of the dye area in Band 6 of the spectrophotography verifies the sensitivity of this technique to surface-condition indication.

The variability of illumination conditions has an important effect in the determination of the spectral reflectance of natural surfaces. In fact, the variation of illumination is likely as important in determining the spectral reflectance of a natural surface as is the composition of the surface itself.

However, work on correlation of reflectance with bearing strength and associated trafficability considerations is limited. Some correlations of this nature are established in this report. More extensive work is needed to make adequate use of the available data-collecting instruments. The sensitivity and capacity of present instrumentation far exceeds the existing ability for optimum interpretation and utilization of the data.

The reported investigations and interpretations prove that spectral reflectance variations due to moisture, density, and compositional differences of soils found in playa materials can be detected and identified by airborne means. When coupled with measurement of playa properties or analogous material, spectrophotography can serve to establish knowledge as to the capability of playas to sustain the operations of vehicles or aircraft. The use of infrared thermal imagery enables the relative differentiation of density and moisture, particularly when day and night imagery are available for comparisons. The tonal changes recorded on the imagery provide relative discrimination of soft, wet, or puffy surfaces as opposed to hard, dry, or crusted surfaces.

Acknowledgments

The AFCRL field party included Mr. Richard W. Dowling and Martin Margarita, A/2, USAF, of the Terrestrial Sciences Laboratory, who performed diligently under adverse conditions of ground temperature and observation times.

Aerial photography was accomplished by Roland E. Hudson, SSgt, USAF, of the same Laboratory, who successfully operated three cameras. Appreciation is expressed to Mr. Taylor Moorman of the NASA Manned Spacecraft Center for the processing of all special film.

Aerial infrared imagery was obtained with the AFCRL M1A1 scanner by personnel of the Infrared Physics Laboratory, Institute of Science and Technology, the University of Michigan, led by Mr. Carl D. Miller, with imagery processing accomplished at the University of Michigan by Mr. Arnold Birko. These cooperative efforts were conducted under contract No. 1224(44) with the Office of Naval Research, jointly funded by AFCRL.

The NC-47J aircraft and associated infrared processing equipments used in the program were made available by the U.S. Army Electronics Command, Fort Monmouth, N.J., on a cost-reimbursement basis. The aircraft is bailed to the University of Michigan in support of Project MICHIGAN, contract DA-28-043 AMC-00013(3), administered by USAECOM.

The passive microwave measurements were conducted by a field party led by Mr. A. T. Edgerton of the Space Division of Aerojet-General Corporation, which provided the instrumented vehicle and services under their contract Nonr. 4767(00) with the Office of Naval Research, jointly funded by AFCRL.

Acknowledgments

Appreciation is expressed to the operations personnel of the AF Flight Test Center for assistance in flight scheduling and basing of the aircraft at Edwards AFB, California.

The multispectral camera used in this program was developed with support given by the AFCRL Laboratory Directors Fund.

References

Aerojet-General Corp. (1968) Passive Microwave Measurements of Snow, Soils, and Snow-Ice-Water Systems, SGD-829-6.

Ashburn, E.V., and Weldon, R.G. (1956) Spectral diffuse reflectance of desert surfaces, J.O.S.A. 46:585.

Bliamptis, E.E., ed. (1967) Remote Sensing of the Geological Environment, AFCRL.

Coulson, K.L. (1966) Effects of Reflection Properties of Natural Surfaces in Aerial Reconnaissance, App. op. 5:905.

Coulson, K.L., Bouricius, G.M., and Gray, E.L. (1965) Optical reflection properties of natural surfaces, J.G.R. 70:4601.

Cronin, J.F. (1967) Terrestrial Multispectral Photography, Special Reports No. 56, AFCRL-67-0076.

Cronin, J.F., Rooney, T.P., Williams, R.S., Jr., Molineux, C.E., and Bliamptis, E.E. (1968) Ultraviolet Radiation and the Terrestrial Surface, Special Reports No. 83, AFCRL-68-0572.

Hapke, B.W. (1963) A theoretical photometric function for the lunar surface, J.G.R. 68:4571.

Hapke, B.W., and Van Horn, H. (1963) Photometric studies of complex surfaces with applications to the moon, J.G.R. 68:4545.

Kennedy, J.M., and Edgerton, A.T. (1968) Microwave Radiometric Sensing of Soil Moisture Content, Publication No. 78, General Assembly of Bern 1967, International Association of Scientific Hydrology.

Kondratyev, K. Ya. (1965) Actinometriya, Leningrad.

Krinov, E.L. (1947) Spectral reflectance properties of natural formations, Akad. Nauk. SSSR, Moscow (1947), Tech. Transl. TT 439, NRC of Canada, Ottawa (1953).

References

Mitchel, R.H. (1969) Applications of Optical Data Processing Techniques to Geological Imagery, Final Contract Report, University of Michigan, AFCRL-69-0386.

Molineux, C.E. (1965) Multiband spectral system for reconnaissance, Photogrammetric Engineering XXXI:1.

Motts, W.S., (ed) (1969) Geology and Hydrology of Selected Playas in Western United States, AFCRL-69-0214.

Neal, J.T. (1963) Geology of Selected Playas, Unpublished AFCRL Report.

Neal, J.T. (ed) (1965) Geology, Mineralogy, and Hydrology of U.S. Playas, Environmental Research Papers No. 96, AFCRL-65-266.

Neal, J.T., Langer, A.M., and Kerr, P.F. (1968) Giant dessication polygons of great basin playas, Geol. Soc. Am. Bull., 69:69-90.

Neal, J.T., (ed) (1968) Playa Surface Morphology: Miscellaneous Investigations, Environmental Research Papers No. 283, AFCRL-68-0133.

Sekera, Z. (1957) in Encyclopedia of Physics, S. Flugge, Ed., Vol. 48.

Spencer, D.E. (1965) Out-of-focus photometry, J.O.S.A. 55:396.

Appendix A

Field Measurement Data

LOCATION		CP23			CP26		
DESCRIPTION		N. End on Slope (gray rise)			Salt Crust		
FILTER		ND3	ND3 HN38 ∥	ND3 HN38 ⊥	ND3	ND3 HN38 ∥	ND3 HN38 ⊥
BAND	1	.025	-	-	.031	-	-
	2	.16	-	-	1.85	-	-
	3	1.12	.39	.405	1.14	.41	.42
	4	1.61	.60	.63	1.48	.56	.58
	5	1.78	.67	.70	1.58	.61	.62
	6	1.35	.50	.52	1.13	.42	.44
	7	1.94	-	-	1.65	-	-
	8	.77	-	-	.65	-	-
	9	.90	-	-	.75	-	-
	10	3.2	-	-	2.70	-	-
START/FINISH		1323/1325			1100/1107		
DATE		9-16-67			9-16-67		
θ_S		49.62°			32.75°		
θ_A		-			-		
θ_D		0.0°			0.0°		

LOCATION		CP27			CP31		
DESCRIPTION		Brown Crust Near Salt Stains			Hard Salt Crust		
FILTER		ND3	ND3 HN38 ∥	ND3 HN38 ⊥	ND3	ND3 HN38 ∥	ND3 HN38 ⊥
BAND	1	.016	.0094	.0062	.032	-	-
	2	.11	.035	.056	.177	-	-
	3	.80	.32	.34	1.22	.43	.42
	4	.91	.47	.525	1.65	.635	.62
	5	1.20	.59	.625	1.84	.61	.70
	6	1.15	.46	.50	1.35	.51	.50
	7	1.88	.72	.76	1.96	-	-
	8	.68	.30	.32	.77	-	-
	9	.84	.38	.42	.90	-	-
	10	3.1	1.57	1.66	3.2	-	-
START/FINISH		1111/1118			1047/1051		
DATE		9-16-67			9-16-67		
θ_S		33.25°			32.39°		
θ_A		-			-		
θ_D		0.0°			0.0°		

LOCATION		CP32			CP32A		
DESCRIPTION		Recent Crack Inside			Recent Crack Outside		
FILTER		ND3	ND3 HN38 ∥	ND3 HN38 ⊥	ND3	ND3 HN38 ∥	ND3 HN38 ⊥
BAND	1	.014	-	-	.0195	-	-
	2	.072	-	-	.11	-	-
	3	.53	.17	.17	.84	.295	.3
	4	.74	.265	.265	1.2	.46	.47
	5	.87	.32	.32	1.41	.55	.56
	6	.705	.25	.25	1.15	.44	.44
	7	1.05	-	-	1.77	-	-
	8	.45	-	-	.74	-	-
	9	.55	-	-	.89	-	-
	10	2.1	-	-	3.4	-	-
START/FINISH		0952/0958			1001/1006		
DATE		9-16-67			9-16-67		
θ_S		34.12°			33.52°		
θ_A		-			-		
θ_D		0.0°			0.0°		

LOCATION		CP34			CP36		
DESCRIPTION		Old Crack			Brown Flaky "Wet Look" Crust		
FILTER		ND3	ND3 HN38 ∥	ND3 HN38 ⊥	ND3	ND3 HN38 ∥	ND3 HN38 ⊥
BAND	1	.0125	-	-	.016	-	-
	2	.0825	-	-	.086	-	-
	3	.69	.22	.25	.67	.22	.23
	4	1.03	.38	.42	.95	.36	.37
	5	1.22	.45	.50	1.15	.42	.44
	6	1.03	.38	.40	.95	.34	.36
	7	1.52	-	-	1.47	-	-
	8	.67	-	-	.58	-	-
	9	.82	-	-	.70	-	-
	10	3.2	-	-	2.6	-	-
START/FINISH		0902/0908			1254/1259		
DATE		9-16-67			9-16-67		
θ_S		39.39°			45.09°		
θ_A					-		
θ_D		0.0°			0.0°		

LOCATION		CP37			CP38		
DESCRIPTION		N. End on Playa			Light "Dry Look" Surface		
FILTER		ND3	ND3 HN38 ∥	ND3 HN38 ⊥	ND3	ND3 HN38 ∥	ND3 HN38 ⊥
BAND	1	.0295	-	-	.03	-	-
	2	.19	-	-	.207	-	-
	3	1.47	.51	.54	1.57	.56	.59
	4	2.12	.80	.84	2.27	.87	.91
	5	2.45	.92	.96	2.58	.99	1.00
	6	1.92	.71	.74	2.07	.79	.77
	7	2.8	-	-	3.00	-	-
	8	1.12	-	-	1.25	-	-
	9	1.34	-	-	1.45	-	-
	10	4.95	-	-	5.7	-	-
START/FINISH		1311/1316			1131/1142		
DATE		9-16-67			9-17-67		
θ_S		47.88°			35.15°		
θ_A		-			-		
θ_D		0.0°			0.0°		

LOCATION		CP39			CP42		
DESCRIPTION		Off N. Edge on Sand			Dye Pattern Near Well		
FILTER		ND3	ND3 HN38 ∥	ND3 HN38 ⊥	ND3	ND3 HN38 ∥	ND3 HN38 ⊥
BAND	1	.0225	-	-	.0115	-	-
	2	.166	-	-	.083	-	-
	3	1.2	.42	.41	.65	.22	.23
	4	1.73	.64	.64	.95	.355	.37
	5	1.94	.73	.72	1.08	.405	.42
	6	1.55	.57	.56	.87	.32	.33
	7	2.3	-	-	1.35	-	-
	8	.93	-	-	.55	-	-
	9	1.13	-	-	.67	-	-
	10	4.1	-	-	2.76	-	-
START/FINISH		1329/1333			0837/0911		
DATE		9-16-67			9-17-67		
θ_S		50.85°					
θ_A		-			-		
θ_D		0.0°			0.0°		

LOCATION		CP42A			CP42B		
DESCRIPTION		Dye Strip 1/2 Purple (Start) ⊥			Dye Strip 1/1 Greenish		
FILTER		ND3	ND3 HN38 ∥	ND3 HN38 ⊥	ND3	ND3 HN38 ∥	ND3 HN38 ⊥
BAND	1	.023	-	-	.02	-	-
	2	.115	-	-	.102	-	-
	3	.81	.275	.275	.75	.26	.26
	4	.96	.36	.36	1.0	.37	.36
	5	.90	.34	.34	1.03	.40	.38
	6	.83	.31	.31	.90	.34	.32
	7	.96	-	-	1.0	-	-
	8	.37	-	-	.35	-	-
	9	.47	-	-	.46	-	-
	10	3.1	-	-	3.0	-	-
START/FINISH		1407/1410			1412/1419		
DATE		9-16-67			9-16-67		
θ_S							
θ_A		-			-		
θ_D		0.0°			0.0°		

LOCATION		CP42C			CP42D		
DESCRIPTION		Dye Strip 3/1 Green			Dye Pattern		
FILTER		ND3	ND3 HN38 ∥	ND3 HN38 ⊥	ND3	ND3 HN38 ∥	ND3 HN38 ⊥
BAND	1	.021	-	-	.011	-	-
	2	.097	-	-	.094	-	-
	3	.70	.25	.24	.76	.24	.25
	4	.96	.37	.36	1.08	.395	.41
	5	1.05	.405	.39	1.25	.46	.48
	6	.87	.33	.32	1.02	.37	.38
	7	.97	-	-	1.35	-	-
	8	.33	-	-	.51	-	-
	9	.44	-	-	.66	-	-
	10	2.82	-	-	2.9	-	-
START/FINISH		1421/1424			1450/1454		
DATE		9-16-67			9-16-67		
θ_S							
θ_A		-			-		
θ_D		0.0°			0.0°		

LOCATION		CP43A			CP43A1		
DESCRIPTION		Wet Area Near Well			Mud Island in Wet Area		
FILTER		ND3	ND3 HN38 ∥	ND3 HN38 ⊥	ND3	ND3 HN38 ∥	ND3 HN38 ⊥
BAND	1	.0049	-	-	.016	-	-
	2	.0283	-	-	.073	-	-
	3	.186	.062	.072	.54	.185	.20
	4	.285	.105	.12	.80	.295	.33
	5	.330	.134	.15	.945	.355	.39
	6	.29	.114	.122	.80	.295	.31
	7	.455	-	-	1.25	-	-
	8	.18	-	-	.52	-	-
	9	.242	-	-	.62	-	-
	10	1.02	-	-	2.42	-	-
START/FINISH		0755/0807			0925/0938		
DATE		9-16-67			9-17-67		
θ_S		49.34°			36.52°		
θ_A		-			-		
θ_D		0.0°			0.0°		

LOCATION		CP43B			CP43B1		
DESCRIPTION		Dry Area Near Well			Dry Area Near Well		
FILTER		ND3	ND3 HN38 ∥	ND3 HN38 ⊥	ND3	ND3 HN38 ∥	ND3 HN38 ⊥
BAND	1	.0073	-	-	.0175	-	-
	2	.0395	-	-	.122	-	-
	3	.32	.126	.135	.93	.31	.33
	4	.495	.202	.216	1.37	.50	.54
	5	.595	.244	.258	1.55	.57	.63
	6	.51	.205	.207	1.23	.45	.46
	7	.745	-	-	1.85	-	-
	8	.31	-	-	.77	-	-
	9	.40	-	-	.86	-	-
	10	1.64	-	-	3.25	-	-
START/FINISH		0809/0815			0941/0953		
DATE		9-16-67			9-17-67		
θ_S		47.45°			35.12°		
θ_A		-			-		
θ_D		0.0°			0.0°		

LOCATION		CP44A			CP44B		
DESCRIPTION		Mud Due to Well Water			Water Stain (Mud)		
FILTER		ND3	ND3 HN38 ∥	ND3 HN38 ⊥	ND3	ND3 HN38 ∥	ND3 HN38 ⊥
BAND	1	.013	-	-	.019	-	-
	2	.072	-	-	.105	-	-
	3	.56	.18	.195	.76	.46	.32
	4	.82	.285	.31	1.07	.57	.48
	5	.96	.34	.365	1.20	.61	.54
	6	.82	.29	.295	.96	.47	.40
	7	1.27	-	-	1.5	-	-
	8	.52	-	-	.61	-	-
	9	.65	-	-	.76	-	-
	10	2.48	-	-	2.88	-	-
START/FINISH		1430/1435			1436/1440		
DATE		9-16-67			9-16-67		
θ_S		62.43°			63.42°		
θ_A		-			300.0°		
θ_D		0.0°			45.0°		

LOCATION		CP45					
DESCRIPTION		Dye Cross Green					
FILTER		ND3	ND3 HN38 ∥	ND3 HN38 ⊥	ND3	ND3 HN38 ∥	ND3 HN38 ⊥
BAND	1	.057	-	-			
	2	.22	-	-			
	3	1.45	.5	.55			
	4	2.05	.75	.82			
	5	2.16	.84	.91			
	6	1.77	.65	.72			
	7	2.35	-	-			
	8	.94	-	-			
	9	1.12	-	-			
	10	5.0	-	-			
START/FINISH		1200/1205					
DATE		9-17-67					
θ_S		-					
θ_A		45.0°					
θ_D		30.0°					

LOCATION		HP29			HP38		
DESCRIPTION		Brown Puffy Crust			Fan Near Playa Edge		
FILTER		ND3	ND3 HN38 ∥	ND3 HN58 ⊥	ND3	ND3 HN38 ∥	ND3 HN38 ⊥
BAND	1	.0132	-	-	.008	-	-
	2	.084	-	-	.068	-	-
	3	.62	.205	.22	.53	-	-
	4	.88	.31	.33	.78	-	-
	5	.99	.365	.38	.89	-	-
	6	.825	.29	.30	.74	-	-
	7	1.2	-	-	1.05	-	-
	8	.52	-	-	.44	-	-
	9	.62	-	-	.55	-	-
	10	2.37	-	-	2.18	-	-
START/FINISH		1204/1211			0830/0837		
DATE		9-14-67			9-14-67		
θ_S		37.02°			43.68°		
θ_A		-			-		
θ_D		0.0°			0.0°		

LOCATION		HP39			HP41		
DESCRIPTION		Playa Crust Near 38			Soft Puffy Ground		
FILTER		ND3	ND3 HN38 ∥	ND3 HN38 ⊥	ND3	ND3 HN38 ∥	ND3 HN38 ⊥
BAND	1	.0075	-	-	.0097	-	-
	2	.057	-	-	.078	-	-
	3	.475	-	-	.62	-	-
	4	.71	-	-	.91	.36	.34
	5	.83	-	-	1.05	.41	.59
	6	.72	-	-	.88	.325	.32
	7	1.05	-	-	1.37	-	-
	8	.44	-	-	.53	-	-
	9	.555	-	-	.64	-	-
	10	2.25	-	-	2.5	-	-
START/FINISH		0847/0855			0922/0929		
DATE		9-14-67			9-14-67		
θ_S		41.07°			36.42°		
θ_A		-			-		
θ_D		0.0°			0.0°		

LOCATION		HP42			HP43		
DESCRIPTION		Hard Crust (Dry)			Soft Puffy Surface		
FILTER		ND3	ND3 HN38 ∥	ND3 HN38 ⊥	ND3	ND3 HN38 ∥	ND3 HN38 ⊥
BAND	1	.011	-	.003	.011	-	-
	2	.072	-	.019	.088	-	-
	3	.78	-	.19	.70	-	-
	4	.84	.32	.31	1.05	.39	.37
	5	.94	.35	.36	1.19	.44	.43
	6	.785	.29	.275	1.0	.35	.35
	7	1.1	-	-	1.53	-	.53
	8	.44	-	-	.62	-	.19
	9	.56	-	-	.74	-	.26
	10	2.5	-	-	2.9	-	1.15
START/FINISH		0903/0913			0934/0944		
DATE		9-14-67			9-14-67		
θ_S		37.50^o			35.02^o		
θ_A		-			-		
θ_D		0.0^o			0.0^o		

LOCATION		HP44			HP45		
DESCRIPTION		Soft Puffy Surface			Soft Puffy Ground		
FILTER		ND3	ND3 HN38 ∥	ND3 HN38 ⊥	ND3	ND3 HN38 ∥	ND3 HN38 ⊥
BAND	1	.15	.165	-	.26	.19	-
	2	1.32	1.46	-	2.72	.57	-
	3	3.2	2.6	-	6.6	4.1	-
	4	3.1	2.6	-	6.9	4.5	-
	5	3.1	2.0	-	6.8	3.5	-
	6	2.1	1.25	-	4.2	2.4	-
	7	2.8	1.30	-	5.7	2.5	-
	8	1.15	.62	-	2.6	1.5	-
	9	1.35	.46	-	2.4	1.0	-
	10	3.7	.72	-	4.2	0.9	-
START/FINISH		1416/1426			1444/1457		
DATE		9-12-67			9-12-67		
θ_S		58.45^o			64.35^o		
θ_A		$+90.0^o$			180.0^o		
θ_D		45.0^o			45.0^o		

LOCATION		HP46			HP47		
DESCRIPTION		Hard Dry Crust			Edge; Light Puffy Area		
FILTER		ND3	ND3 HN38 ∥	ND3 HN38 ⊥	ND3	ND3 HN38 ∥	ND3 HN38 ⊥
BAND	1	.0092	-	-	.13	-	-
	2	.075	-	-	1.15	-	-
	3	.57	.17	.17	3.0	-	-
	4	.85	.30	.31	3.0	-	-
	5	.95	.34	.36	3.1	-	-
	6	.82	.28	.29	2.1	-	-
	7	1.25	-	-	2.8	-	-
	8	0.5	-	-	1.1	-	-
	9	.58	-	-	1.2	-	-
	10	2.45	-	-	3.6	-	-
START/FINISH		0951/0958			1504/1509		
DATE		9-14-67			9-12-67		
θ_S		33.58°			67.53°		
θ_A		-			+90.0°		
θ_D		0.0°			45.0°		

LOCATION		HP48			HP55		
DESCRIPTION		Light Puffy Area			Self Rising Puffy Crust		
FILTER		ND3	ND3 HN38 ∥	ND3 HN38 ⊥	ND3	ND3 HN38 ∥	ND3 HN38 ⊥
BAND	1	.10	-	-	.008	.0076	.004
	2	.92	-	-	.018	.022	.018
	3	2.45	-	-	.42	.18	.16
	4	2.46	-	-	.63	.27	.27
	5	2.51	-	-	.74	.30	.31
	6	1.65	-	-	.64	.25	.26
	7	2.31	-	-	1.0	-	-
	8	.96	-	-	.40	-	-
	9	.32	-	-	.49	-	-
	10	3.1	-	-	2.1	-	-
START/FINISH		1510/1515			1046/1054		
DATE		9-12-67			9-14-67		
θ_S		68.75°			31.77°		
θ_A		+270.0°			-		
θ_D		45.0°			0.0°		

LOCATION		HP56					
DESCRIPTION		Salt Stained Mud					
FILTER		ND3	ND3 HN38 ∥	ND3 HN38 ⊥	ND3	ND3 HN38 ∥	ND3 HN38 ⊥
BAND	1	.015	-	-			
	2	.09	-	-			
	3	.70	-	-			
	4	.97	.37	.37			
	5	1.06	.41	.41			
	6	.89	.33	.32			
	7	1.33	-	-			
	8	.55	-	-			
	9	.64	-	-			
	10	2.55	-	-			
START/FINISH		1031/1042					
DATE		9-14-67					
θ_S		31.63°					
θ_A		-					
θ_D		0.0°					

LOCATION		NP8A			NP8B		
DESCRIPTION		Alluvial Fan Dark			Alluvial Fan Dark ⊥		
FILTER		ND3	ND3 HN38 ∥	ND3 HN38 ⊥	ND3	ND3 HN38 ∥	ND3 HN38 ⊥
BAND	1	.11	.092	.075	.0116	-	-
	2	1.1	.92	.82	.078	-	-
	3	2.77	2.3	1.87	.53	.177	.19
	4	2.55	1.97	1.64	.75	.261	.23
	5	2.57	2.01	1.63	.81	.281	.27
	6	1.30	.97	.71	.63	.214	.237
	7	1.72	1.2	.94	.89	.26	.27
	8	.76	.55	.44	.33	-	-
	9	.75	.47	.41	.41	-	-
	10	1.30	.59	.65	1.61	-	-
START/FINISH		0800/0810			0942/0952		
DATE		9-15-67			9-15-67		
θ_S		49.58°			34.80°		
θ_A		90.0°			-		
θ_D		70.0°			0.0°		

LOCATION		NP9A			NP9B		
DESCRIPTION		Hard Light Area. Near NP8			Hard Light Area ⊥		
FILTER		ND3	ND3 HN38 ∥	ND3 HN38 ⊥	ND3	ND3 HN38 ∥	ND3 HN38 ⊥
BAND	1	.087	-	-	.0186	.0054	.0035
	2	.72	-	-	.13	.035	.032
	3	2.55	-	-	.94	.30	.29
	4	2.61	-	-	1.35	.47	.49
	5	2.70	-	-	1.51	.54	.57
	6	1.55	-	-	1.25	.41	.46
	7	2.17	-	-	1.82	.61	.67
	8	.84	-	-	.78	.22	.25
	9	.90	-	-	.92	.30	.35
	10	2.77	-	-	3.30	1.32	1.45
START/FINISH		0813/0820			0956/1006		
DATE		9-15-67			9-15-67		
θ_S		47.58°			34.10°		
θ_A		90.0°			-		
θ_D		70.0°			0.0°		

LOCATION		NP10			NP11		
DESCRIPTION		Hard Light Area. Flat			Sandfinger. Near NP10		
FILTER		ND3	ND3 HN38 ∥	ND3 HN38 ⊥	ND3	ND3 HN38 ∥	ND3 HN38 ⊥
BAND	1	.019	-	-	.014	-	-
	2	.142	-	-	.095	-	-
	3	1.0	.35	.38	.735	.22	.22
	4	1.47	.54	.60	.95	.35	.39
	5	1.66	.62	.67	1.1	.41	.45
	6	1.35	.49	.53	.88	.32	.34
	7	2.0	-	-	1.33	-	-
	8	.77	-	-	.56	-	-
	9	.95	-	-	.68	-	-
	10	3.6	-	-	2.55	-	-
START/FINISH		1011/1016			1019/1025		
DATE		9-15-67			9-15-67		
θ_S		33.72°			33.32°		
θ_A		-			-		
θ_D		0.0°			0.0°		

LOCATION		NP12			NP13		
DESCRIPTION		Dark Area			Light Area. Near NP12		
FILTER		ND3	ND3 HN38 ∥	ND3 HN38 ⊥	ND3	ND3 HN38 ∥	ND3 HN38 ⊥
BAND	1	.012	-	-	.016	-	-
	2	.067	-	-	.115	-	-
	3	.54	.155	.18	.90	.28	.31
	4	.76	.25	.28	1.22	.435	.49
	5	.92	.31	.34	1.43	.51	.565
	6	.80	.26	.28	1.15	.40	.44
	7	1.14	-	-	1.66	-	-
	8	.48	-	-	.69	-	-
	9	.61	-	-	.86	-	-
	10	2.42	.	.	3.10	-	-
START/FINISH		1037/1043			1045/1051		
DATE		9-15-67			9-15-67		
θ_S		33.32°			33.57°		
θ_A		-			-		
θ_D		0.0°			0.0°		

LOCATION		NP14A			NP14B		
DESCRIPTION		Dark Flaky Crust			Ceramic Tiles, NP14A ⊥		
FILTER		ND3	ND3 HN38 ∥	ND3 HN38 ⊥	ND3	ND3 HN38 ∥	ND3 HN38 ⊥
BAND	1	.01	-	-	.0375	-	-
	2	.255	-	-	.13	-	-
	3	1.55	.41	.58	1.00	.29	.32
	4	2.00	.59	.84	1.44	.49	.51
	5	2.00	.59	.84	1.65	.56	.58
	6	1.42	.41	.58	1.35	.44	.45
	7	1.90	-	-	1.90	-	-
	8	.73	-	-	.77	-	-
	9	.92	-	-	1.00	-	-
	10	3.40	-	-	3.90	-	-
START/FINISH		1100/1105			1113/1116		
DATE		9-15-67			9-15-67		
θ_S		33.82°			35.25°		
θ_A		150.0°			-		
θ_D		80.0°			0.0°		

LOCATION		NP16A			NP16B		
DESCRIPTION		Dark Alluvial Wash ⊥			Dark Alluvial Wash		
FILTER		ND3	ND3 HN38 ∥	ND3 HN38 ⊥	ND3	ND3 HN38 ∥	ND3 HN38 ⊥
BAND	1	.013	-	-	.021	-	-
	2	.095	-	-	.105	-	-
	3	.72	-	-	.62	.19	.15
	4	1.04	-	-	.80	.28	.23
	5	1.18	-	-	.82	.26	.31
	6	.98	-	-	.64	.21	.18
	7	1.44	-	-	.88	-	-
	8	.56	-	-	.35	-	-
	9	.75	-	-	.46	-	-
	10	3.0	-	-	1.78	-	-
START/FINISH		1133/1136			1138/1144		
DATE		9-15-67			9-15-67		
θ_S		35.73°			39.25		
θ_A		-			30.0°		
θ_D		0.0°			85.0°		

LOCATION		SP3			SP5		
DESCRIPTION		Self Rising Ground			Salt Stained Porous Crust		
FILTER		ND3	ND3 HN38 ∥	ND3 HN38 ⊥	ND3	ND3 HN38 ∥	ND3 HN38 ⊥
BAND	1	.16	-	-	.16	-	-
	2	1.2	-	-	1.37	-	-
	3	3.0	-	-	3.5	-	-
	4	2.5	-	-	3.3	-	-
	5	2.6	-	-	3.3	-	-
	6	1.3	-	-	2.05	-	-
	7	1.7	-	-	2.45	-	-
	8	.5	-	-	1.1	-	-
	9	.5	-	-	1.1	-	-
	10	1.6	-	-	2.8	-	-
START/FINISH		0956/1000			1036/1040		
DATE		9-13-67			9-15-67		
θ_S		33.92°			32.27°		
θ_A		215.0°			90.0°		
θ_D		45.0°			45.0°		

LOCATION		SP6			SP7		
DESCRIPTION		Light Hard Crust			Light Hard Crust		
FILTER		ND3	ND3 HN38 ∥	ND3 HN38 ⊥	ND3	ND3 HN38 ∥	ND3 HN38 ⊥
BAND	1	.188	-	-	.28	-	-
	2	1.50	-	-	2.70	-	-
	3	3.40	-	-	-	-	-
	4	3.10	-	-	-	-	-
	5	3.30	-	-	-	-	-
	6	1.90	-	-	-	-	-
	7	2.50	-	-	-	-	-
	8	1.0	-	-	-	-	-
	9	1.0	-	-	-	-	-
	10	3.1	-	-	-	-	-
START/FINISH		1002/1004			1004/1007		
DATE		9-13-67			9-13-67		
θ_S		33.63°			33.43°		
θ_A		30.0°			300.0°		
θ_D		45.0°			45.0°		

LOCATION		SP8			SP10		
DESCRIPTION		Self Rising Ground Dark			Light White Area		
FILTER		ND3	ND3 HN38 ∥	ND3 HN38 ⊥	ND3	ND3 HN38 ∥	ND3 HN38 ⊥
BAND	1	.34	-	-	.0032	-	-
	2	3.6	-	-	.012	-	-
	3	9.3	-	-	.07	.0305	.028
	4	9.1	-	-	.089	.04	.038
	5	off scale 10^+	-	-	.092	.041	.038
	6	6.2	-	-	.072	.031	.0285
	7	8.8	-	-	.095	-	-
	8	4.5	-	-	.04	-	-
	9	4.2	-	-	.049	-	-
	10	4.0	-	-	.19	-	-
START/FINISH		1009/1013			1417/1421		
DATE		9-13-67			9-15-67		
θ_S		33.10°			59.38°		
θ_A		300.0°			90.0°		
θ_D		45.0°			75.0°		

LOCATION		SP11			SP12		
DESCRIPTION		Salt Crusted Area			Dark Brown Area		
FILTER		ND3	ND3 HN38 ∥	ND3 HN38 ⊥	ND3	ND3 HN38 ∥	ND3 HN38 ⊥
BAND	1	.0058	-	-	.0037	-	-
	2	.025	-	-	.012	-	-
	3	.14	.052	.031	.053	.019	.018
	4	.18	.071	.070	.064	.024	.023
	5	.18	.071	.069	.063	.024	.022
	6	.13	.052	.050	.046	.017	.016
	7	.105	-	-	.059	-	-
	8	.07	-	-	.025	-	-
	9	.087	-	-	.029	-	-
	10	.31	-	-	.105	-	-
START/FINISH		1424/1428			1429/1433		
DATE		9-15-67			9-15-67		
θ_S		60.70°			61.67°		
θ_A		90.0°			90.0°		
θ_D		80.0°			83.0°		

LOCATION		SP13					
DESCRIPTION		Light Tan Area					
FILTER		ND3	ND3 HN38 ∥	ND3 HN38 ⊥	ND3	ND3 HN38 ∥	ND3 HN38 ⊥
BAND	1	.0017	-	-			
	2	.095	-	-			
	3	.057	.019	.02			
	4	.068	.025	.027			
	5	.069	.026	.028			
	6	.054	.02	.021			
	7	.072	-	-			
	8	.0295	-	-			
	9	.037	-	-			
	10	.14	-	-			
START/FINISH		1435/1439					
DATE		9-15-67					
θ_S		62.82°					
θ_A		90.0°					
θ_D		85.0°					